

Basigin Promotes Cardiac Fibrosis and Failure in Response to Chronic Pressure Overload in Mice

Kota Suzuki, Kimio Satoh, Shohei Ikeda, Shinichiro Sunamura, Tomohiro Otsuki, Taiju Satoh, Nobuhiro Kikuchi, Junichi Omura, Ryo Kurosawa, Masamichi Nogi, Kazuhiko Numano, Koichiro Sugimura, Tatsuo Aoki, Shunsuke Tatebe, Satoshi Miyata, Rupak Mukherjee, Francis G. Spinale, Kenji Kadomatsu, Hiroaki Shimokawa

Objective—Basigin (Bsg) is a transmembrane glycoprotein that activates matrix metalloproteinases and promotes inflammation. However, the role of Bsg in the pathogenesis of cardiac hypertrophy and failure remains to be elucidated. We examined the role of Bsg in cardiac hypertrophy and failure in mice and humans.

Approach and Results—We performed transverse aortic constriction in *Bsg*^{+/-} and in wild-type mice. *Bsg*^{+/-} mice showed significantly less heart and lung weight and cardiac interstitial fibrosis compared with littermate controls after transverse aortic constriction. Both matrix metalloproteinase activities and oxidative stress in loaded left ventricle were significantly less in *Bsg*^{+/-} mice compared with controls. Echocardiography showed that *Bsg*^{+/-} mice showed less hypertrophy, less left ventricular dilatation, and preserved left ventricular fractional shortening compared with littermate controls after transverse aortic constriction. Consistently, *Bsg*^{+/-} mice showed a significantly improved long-term survival after transverse aortic constriction compared with *Bsg*^{+/+} mice, regardless of the source of bone marrow (*Bsg*^{+/+} or *Bsg*^{+/-}). Conversely, cardiac-specific Bsg-overexpressing mice showed significantly poor survival compared with littermate controls. Next, we isolated cardiac fibroblasts and examined their responses to angiotensin II or mechanical stretch. Both stimuli significantly increased Bsg expression, cytokines/chemokines secretion, and extracellular signal-regulated kinase/Akt/JNK activities in *Bsg*^{+/+} cardiac fibroblasts, all of which were significantly less in *Bsg*^{+/-} cardiac fibroblasts. Consistently, extracellular and intracellular Bsg significantly promoted cardiac fibroblast proliferation. Finally, serum levels of Bsg were significantly elevated in patients with heart failure and predicted poor prognosis.

Conclusions—These results indicate the crucial roles of intracellular and extracellular Bsg in the pathogenesis of cardiac hypertrophy, fibrosis, and failure in mice and humans. (*Arterioscler Thromb Vasc Biol.* 2016;36:636-646. DOI: 10.1161/ATVBAHA.115.306686.)

Key Words: angiotensin II ■ cytokines ■ heart failure ■ hypertrophy ■ inflammation

Heart failure is a major cause of death worldwide.¹ Despite the recent development in medical therapy, the morbidity and mortality rate in patients with heart failure remains high and fundamental treatment remains to be developed. Cardiac dysfunction is caused by excessive fibrosis, hypertrophy, and inflammation.² Pressure overload, such as systemic hypertension and stenotic valvular heart diseases, induces cardiac hypertrophy. Although cardiac hypertrophy is basically a compensatory response to maintain wall stress and cardiac output, sustained hypertrophic response eventually leads to cardiac dysfunction and failure.^{3,4} To date, the mechanism responsible for transition from adaptive cardiac hypertrophy to failure remains to be elucidated. The responses of cardiac tissues to pressure overload are mediated by various

intracellular signaling pathways, including mitogen-activated protein kinase, calcium, inflammation, and oxidative stress-mediated signaling pathways.⁵⁻⁸ We also have demonstrated that these pathways are substantially involved in the development of heart failure.⁹⁻¹¹

Basigin (Bsg, also known as CD147 or EMMPRIN, encoded by *Basigin*) is a transmembrane glycoprotein that is ubiquitously expressed in the body.¹² Bsg is a multifunctional protein that promotes myofibroblast differentiation, cell proliferation, and matrix metalloproteinase (MMP) activation and inhibits autophagy.¹³⁻¹⁵ Bsg is an essential receptor for multiple ligands such as malaria, cyclophilin A (CyPA), and soluble Bsg (sBsg) itself.¹⁶⁻¹⁹ Bsg promotes progressions of several kinds of malignant tumors and collagen diseases.²⁰⁻²²

Received on: October 8, 2015; final version accepted on: February 16, 2016.

From the Department of Cardiovascular Medicine, Tohoku University Graduate School of Medicine, Sendai, Japan (K.S., K.S., S.I., S.S., T.O., T.S., N.K., J.O., R.K., M.N., K.N., K.S., T.A., S.T., H.S.); Division of Cardiothoracic Surgery, Medical University of South Carolina, Charleston (R.M.); Department of Cell Biology and Anatomy, University of South Carolina School of Medicine, Columbia (F.G.S.); and Department of Biochemistry, Nagoya University Graduate School of Medicine, Nagoya, Japan (K.K.).

This manuscript was sent to Qingbo Xu, Consulting Editor, for review by expert referees, editorial decision, and final disposition.

The online-only Data Supplement is available with this article at <http://atvb.ahajournals.org/lookup/suppl/doi:10.1161/ATVBAHA.115.306686/-DC1>.

Correspondence to Hiroaki Shimokawa, MD, PhD, Department of Cardiovascular Medicine, Tohoku University Graduate School of Medicine, Sendai 980-8574, Japan. E-mail shimo@cardio.med.tohoku.ac.jp

© 2016 American Heart Association, Inc.

Arterioscler Thromb Vasc Biol is available at <http://atvb.ahajournals.org>

DOI: 10.1161/ATVBAHA.115.306686

Nonstandard Abbreviations and Acronyms

Ang II	angiotensin II
Bsg	basigin
CF	cardiac fibroblast
Col1a	collagen 1a
CyPA	cyclophilin A
IL	interleukin
MMP	matrix metalloproteinase
NRCM	neonatal rat cardiomyocyte
TAC	transverse aortic constriction

In the cardiovascular field, Bsg promotes pulmonary hypertension, atherosclerosis, and platelets activation.^{15,16,23–25} Bsg also disrupts nitric oxide metabolism and causes harmful endothelial activation, including the Rho/Rho-kinase activation.²⁶ Importantly, Bsg is highly expressed in the left ventricle (LV) in patients with dilated cardiomyopathy, myocardial infarction, and inflammatory cardiomyopathy.^{27–29} However, the role of Bsg expression in the pathogenesis of heart failure remains to be elucidated.

In this study, we performed transverse aortic constriction (TAC) in both Bsg knockout (*Bsg*^{−/−}) and cardiomyocyte-specific Bsg-overexpressing mice (Bsg-Tg) to elucidate the role of Bsg in pressure overload–induced heart failure. Here, we report that *Bsg*^{+/-} mice showed resistance to pressure overload and that Bsg-Tg mice showed weakness to pressure overload. Consistently, plasma levels of sBsg was significantly increased in patients with heart failure and well correlated with their long-term survival. Our data suggest that cell surface Bsg and cleaved form of free Bsg (sBsg) are novel therapeutic targets for heart failure.

Materials and Methods

Materials and Methods are available in the online-only Data Supplement.

Results

Bsg in Cardiac Tissue Promotes Cardiac Hypertrophy and Failure

First, we performed TAC in *Bsg*^{+/-} mice and littermate controls (*Bsg*^{+/+} mice) to examine the role of Bsg in the progression of pressure overload–induced heart failure. Because complete Bsg disruption in mice results in perinatal lethality, we used *Bsg*^{+/-} mice in this study. At baseline, there was no difference in blood pressure or heart rate between *Bsg*^{+/-} and *Bsg*^{+/+} mice (Figure 1A). Bsg expression in heart homogenates was reduced by 64% in *Bsg*^{+/-} mice compared with *Bsg*^{+/+} mice (Figure 1A in the online-only Data Supplement). Transverse aortic velocities were comparable between *Bsg*^{+/+} and *Bsg*^{+/-} mice after TAC (Figure 1B in the online-only Data Supplement). In contrast, survival curves demonstrated a significantly less mortality rate in *Bsg*^{+/-} mice compared with *Bsg*^{+/+} mice after TAC (Figure 1B). Echocardiographic examination showed that TAC caused LV dilation and dysfunction in both genotypes (Figure 1C). TAC caused cardiac hypertrophy as examined by interventricular septum and LV posterior

wall thickness in both the genotypes, and the increase in wall thickness was significantly less in *Bsg*^{+/-} compared with *Bsg*^{+/+} mice (Figure 1D). In addition, the increase in LV internal diameter in diastole and the decrease in LV fractional shortening were significantly less severe in *Bsg*^{+/-} compared with *Bsg*^{+/+} mice (Figure 1D). Consistently, the measurement of organ weights showed that TAC significantly increased the ratio of heart weight/body weight and lung weight/body weight in both the genotypes (Figure 1E). Again, the increase in heart/lung weight ratio was significantly less in *Bsg*^{+/-} compared with *Bsg*^{+/+} mice, suggesting that Bsg plays a crucial role in the development of cardiac hypertrophy and failure in response to pressure overload.

Because Bsg plays a crucial role in inflammatory cells that contribute to the development of cardiovascular diseases, we next performed bone marrow (BM) transplantation to examine the role of Bsg in inflammatory cells after TAC. *Bsg*^{+/-} and *Bsg*^{+/+} mice were irradiated and thereafter transplanted with BM cells (*Bsg*^{+/-} or *Bsg*^{+/+}). After reconstitution of BM, mice were subjected to TAC and followed for 4 weeks (Figure 1C in the online-only Data Supplement). Importantly, the expression of Bsg was strong in cardiomyocytes and fibrotic tissue but not in green fluorescent protein⁺ transplanted BM (inflammatory cells; Figure 1D in the online-only Data Supplement). Moreover, *Bsg*^{+/-} recipient mice were more likely to survive compared with *Bsg*^{+/+} recipient mice regardless the source of BM (Figure 1E in the online-only Data Supplement). These data implicated a limited role of Bsg in inflammatory cells of cardiac tissues.

Bsg Augments Pressure Overload–Induced Oxidative Stress and Matrix Metalloproteinase

Because Bsg in cardiac tissue seems to play a crucial role in pressure overloaded heart, we next examined the expression and localization of Bsg in LV after TAC in *Bsg*^{+/-} mice by immunofluorescence staining. Bsg was weakly expressed especially in the interstitial tissue at baseline (Figure 2A; Figure II in the online-only Data Supplement). In contrast, TAC strongly induced Bsg expression in LV in a time-dependent manner, especially in the surface of cardiomyocytes and fibroblasts. Furthermore, Bsg was significantly glycosylated after TAC compared with SHAM control (Figure VA in the online-only Data Supplement). Because Bsg is known to induce inflammation and MMP activation, we further evaluated TAC-mediated induction of oxidative stress (Figure 2B; Figure III in the online-only Data Supplement) and activation of MMPs (Figure 2C; Figure IV in the online-only Data Supplement). Dihydroethidium staining of the LV showed that oxidative stress was induced in both genotypes in a time-dependent manner. However, the extent of oxidative stress in the LV was less in *Bsg*^{+/-} compared with *Bsg*^{+/+} (Figure 2B). In situ zymography (DQ gelatin) showed that MMP activation in the LV was significantly attenuated in *Bsg*^{+/-} compared with *Bsg*^{+/+} (Figure 2C; Figure IV in the online-only Data Supplement). MMP activities as examined by gelatin zymography were also significantly less in *Bsg*^{+/-} LV homogenates than in *Bsg*^{+/+} LV homogenates (Figure 2D). Thus, Bsg plays a crucial role in pressure overload–induced oxidative stress and MMP activation in the LV.

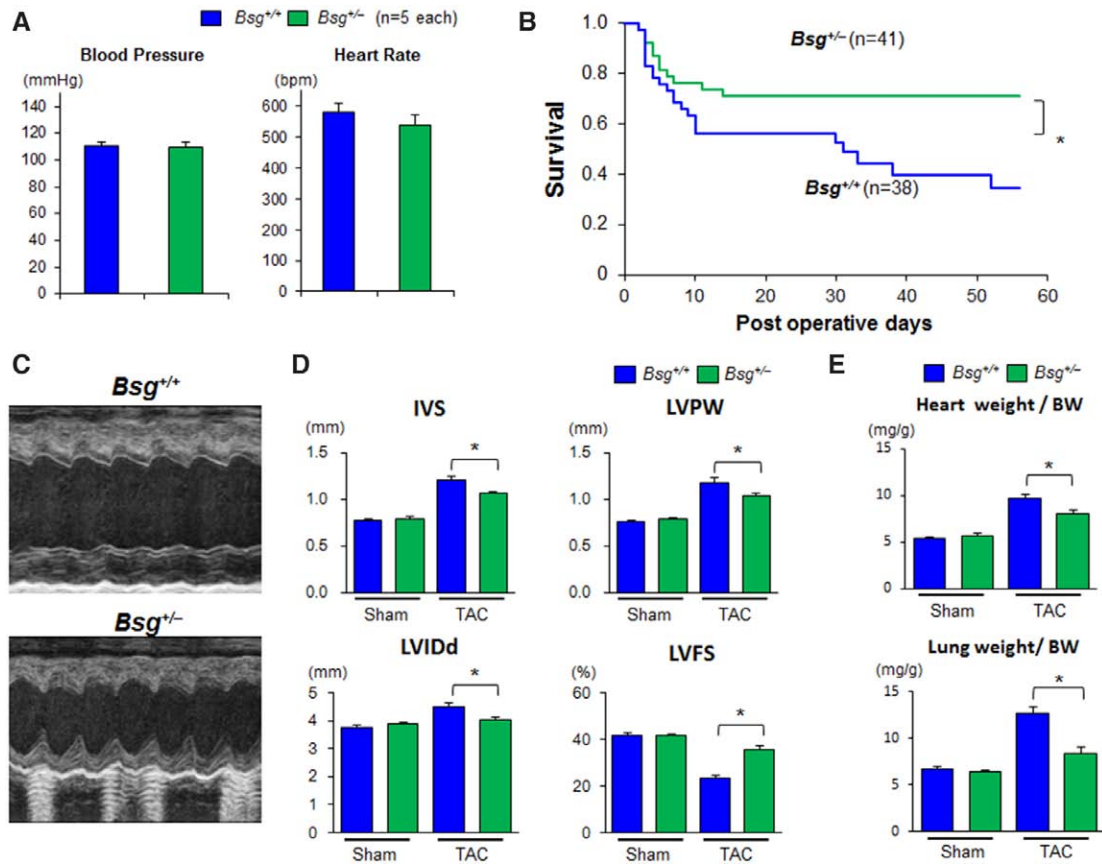


Figure 1. Basigin (Bsg) promotes pressure overload-induced cardiac hypertrophy and failure. **A**, Heart rate and blood pressure measured by tail-cuff method in $Bsg^{+/-}$ and $Bsg^{+/+}$ mice ($n=4$ in each group). **B**, Long-term survival curves showed that mortality rate was significantly ameliorated in $Bsg^{+/-}$ ($n=41$) compared with $Bsg^{+/+}$ mice ($n=38$) after transverse aortic constriction (TAC). **C**, Representative transthoracic M-mode echocardiographic tracing of the heart in $Bsg^{+/-}$ and $Bsg^{+/+}$ mice 4 weeks after TAC. **D**, Quantitative analysis of the parameters of cardiac function in $Bsg^{+/-}$ and $Bsg^{+/+}$ mice at 4 weeks after TAC ($n=8$ in each group). **E**, Ratio of heart weight to body weight (BW) and lung weight to BW in $Bsg^{+/-}$ and $Bsg^{+/+}$ mice at 4 weeks after TAC ($n=8$ in each group). Results are expressed as mean \pm SEM. IVS indicates interventricular septum thickness; LVFS, left ventricular fractional shortening; LVIdD, LV internal end-diastolic diameter; and LVPW, LV posterior wall thickness. * $P<0.05$.

Bsg Promotes Cardiac Fibrosis and Inflammation by Pressure Overload

We next performed histological analyses in $Bsg^{+/-}$ and $Bsg^{+/+}$ mice. Elastica–Masson staining demonstrated that TAC induced interstitial fibrosis in the LV of both genotypes (Figure 3A). However, the extent of increase was significantly less in $Bsg^{+/-}$ compared with $Bsg^{+/+}$ mice at 4 weeks after TAC (Figure 3A). Importantly, immunohistochemistry showed that the expression of CyPA, a potent oxidative stress and inflammation inducer, was increased in $Bsg^{+/+}$ LVs compared with $Bsg^{+/-}$ LVs after TAC (Figure 3B). The expression of CyPA and its receptor, Bsg, was colocalized in the LVs after TAC (Figure 3B), suggesting the crucial role of the CyPA/Bsg signaling in the development of cardiac fibrosis and inflammation in pressure overload-induced heart failure. In addition, α -smooth muscle actin expression in the LV was markedly less in $Bsg^{+/-}$ compared with $Bsg^{+/+}$ mice after TAC, suggesting an importance of Bsg for myofibroblast activation and cardiac fibrosis (Figure 3B). Consistently, gene expressions of fibrotic markers such as collagen 1a (Col1a) and connective tissue growth factor were significantly less in heart homogenates in $Bsg^{+/-}$ compared with $Bsg^{+/+}$ mice after TAC (Figure 3C).

We further examined induction of inflammatory cytokines in response to TAC. Notably, interleukin (IL)-6 expression in the LV after TAC was significantly less in $Bsg^{+/-}$ compared with $Bsg^{+/+}$ mice, though there were no differences in IL-1 β and tumor necrotic factor- α (Figure 3D). Next, we performed Western blotting to examine the signaling mechanism in $Bsg^{+/+}$ and $Bsg^{+/-}$ hearts after TAC. However, the activities of extracellular signal-regulated kinase, Akt, and stress-activated protein kinase were comparable between $Bsg^{+/+}$ and $Bsg^{+/-}$ hearts after TAC (Figure VB in the online-only Data Supplement). We further examined the Nox expression in hearts after TAC. The Nox2 expression was comparable between $Bsg^{+/-}$ and $Bsg^{+/+}$ hearts at baseline. However, the expressions of Nox2 was significantly less in $Bsg^{+/-}$ hearts compared with $Bsg^{+/+}$ hearts 1 week after TAC (Figure VC and VD in the online-only Data Supplement).

Bsg Activates Cardiac Fibroblasts in Response to Mechanical Stretch and Angiotensin II

There was a significant difference in the severity of cardiac fibrosis between $Bsg^{+/-}$ and $Bsg^{+/+}$ mice after TAC. Thus, we harvested cardiac fibroblasts (CFs) from $Bsg^{+/-}$ and $Bsg^{+/+}$ LV

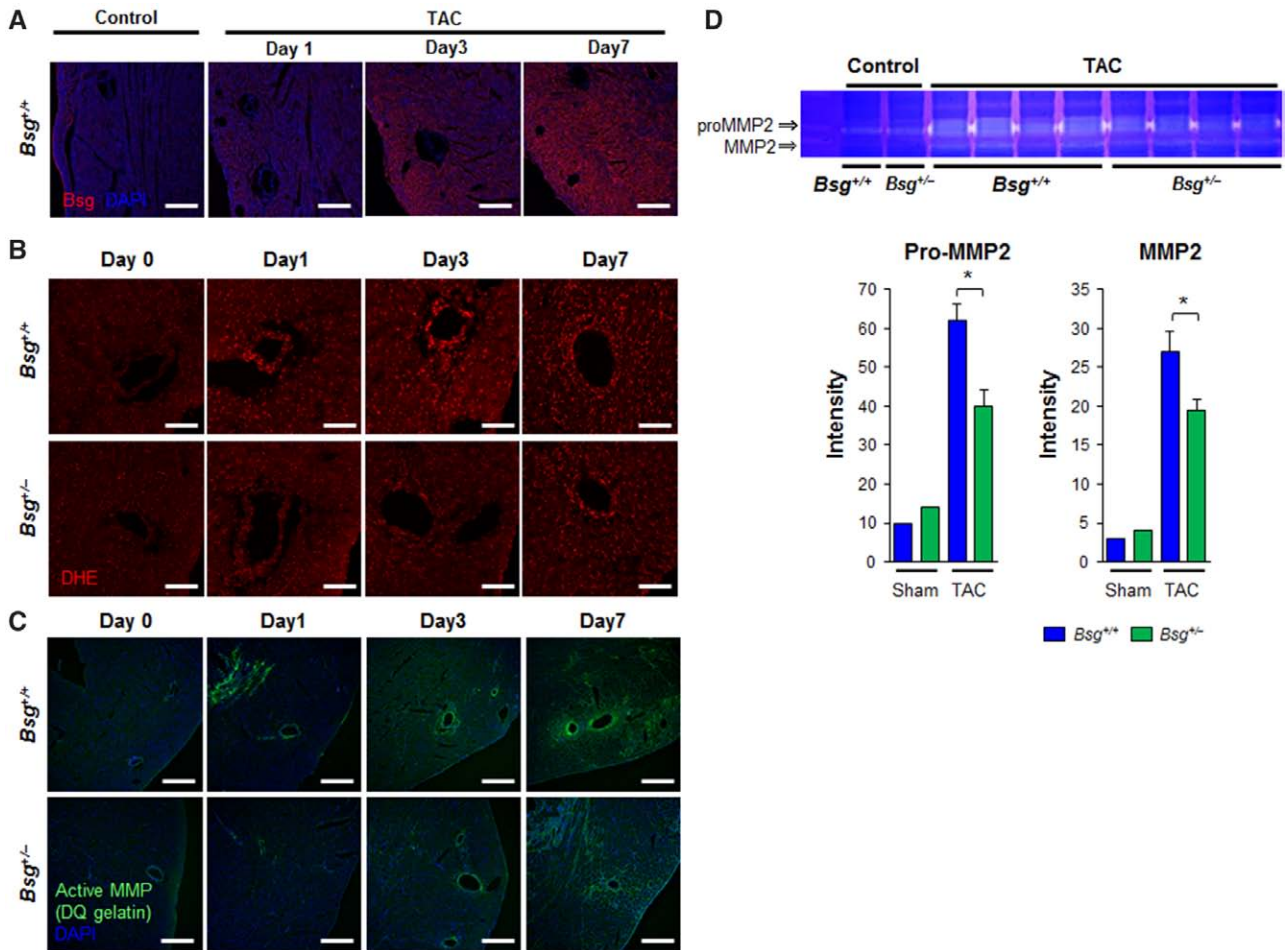


Figure 2. Basigin (Bsg) augments pressure overload–induced oxidative stress and matrix metalloproteinase (MMP) activities. **A**, Representative immunostaining of the left ventricle (LV) after transverse aortic constriction (TAC). Bsg (Alexa Fluor-563, red) and 4',6-diamidino-2-phenylindole (DAPI; blue) expression in the LV after TAC. TAC induced Bsg expression in the LV in a time-dependent manner, especially on the surface of cardiomyocytes. Scale bars, 200 μ m. **B**, Representative pictures of dihydroethidium (DHE) staining of the LV after TAC. Scale bars, 600 μ m. **C**, Representative pictures of in situ zymography (DQ gelatin) for gelatinase activities in the LV after TAC. Scale bars, 300 μ m. **D**, Gelatin zymography to detect proMMP-2 and MMP-2 in heart homogenates at 1 week after TAC. Results are expressed as mean \pm SEM. * P <0.05.

and stimulated them with cyclic mechanical stretch (1 Hz, 20% elongation) or angiotensin II (Ang II; 100 nmol/L) for \leq 24 hours. Cyclic mechanical stretch–activated protein kinase B (Akt) and stress-activated protein kinase in *Bsg*^{+/+} CFs, which was significantly less in *Bsg*^{-/-} CFs (Figure 4A). Interestingly, cyclic mechanical stretch induced Bsg expression in and secretion from CFs, which was significantly less in *Bsg*^{-/-} compared with *Bsg*^{+/+}. CyPA secretion was also significantly less in *Bsg*^{-/-} CFs compared with *Bsg*^{+/+} CFs (Figure 4B). Because Bsg is known as a strong inducer of inflammation, we next examined the secretion of cytokines/chemokines and growth factors from CFs (Figure 4C; Figure VI in the online-only Data Supplement). Importantly, mechanical stretch significantly promoted secretion of several cytokines/chemokines and growth factors in *Bsg*^{+/+} CFs, which was significantly less in *Bsg*^{-/-} CFs, especially for monocyte chemoattractant protein-1, tumor necrotic factor- α , IL-1, IL-18, and monokine induced by γ -interferon (Figure 4C; Figure VI in the online-only Data Supplement). Because pressure overload upregulates Ang II in cardiac tissues, CFs were subjected to Ang II for \leq 24 hours. Again, Ang II significantly activated

Akt, extracellular signal–regulated kinase and stress-activated protein kinases in *Bsg*^{+/+} CFs, which was significantly less in *Bsg*^{-/-} CFs (Figure 4D). Bsg expression and secretion from CFs were significantly less in *Bsg*^{-/-} CFs compared with *Bsg*^{+/+} CFs (Figure 4E). In addition, Ang II significantly promoted secretion of cytokines/chemokines and growth factors from *Bsg*^{+/+} CFs, which was significantly less in *Bsg*^{-/-} CFs, especially for IL-6, IL-17, IL-18, tumor necrotic factor- α , and monokine induced by γ -interferon (Figure 4F and Figure VII in the online-only Data Supplement). These findings suggest that Bsg plays a pivotal role in mediating mechanical stretch- and Ang II–induced CFs activation and inflammation.

Because we found that both mechanical stretch and Ang II promoted significant secretion of Bsg from CFs, we next examined the role of extracellular Bsg. Human recombinant Bsg (hrBsg) significantly activated Akt and extracellular signal–regulated kinase in *Bsg*^{+/+} CFs compared with controls (Figure 5A). Moreover, hrBsg induced atrial natriuretic peptide expression in neonatal rat cardiomyocytes (NRCM; Figure 5B). Furthermore, Bsg knockdown by siRNA significantly reduced Nox2 in neonatal rat CFs (Figure 5C).

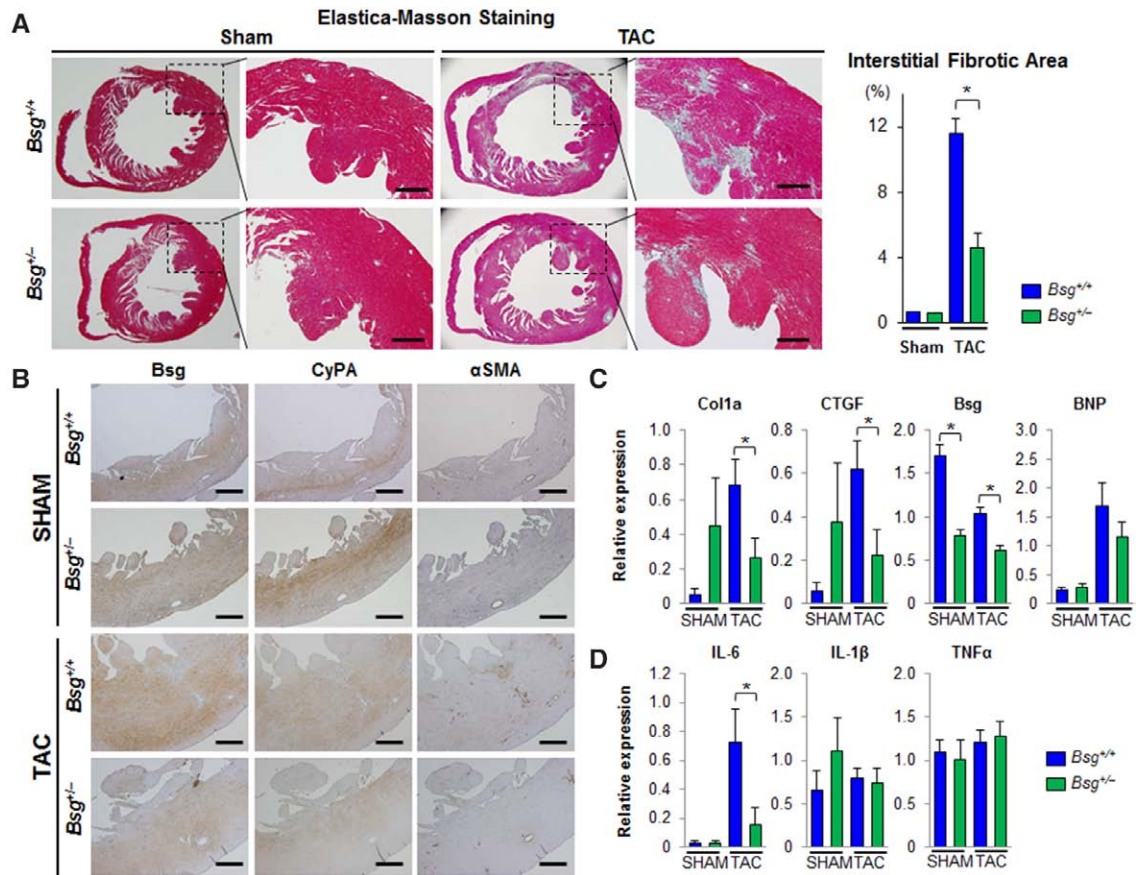


Figure 3. Basigin (Bsg) promotes pressure overload–induced cardiac fibrosis and inflammation. **A**, Representative photomicrographs of Elastica–Masson staining of hearts from *Bsg*^{+/-} and *Bsg*^{+/+} mice at 4 weeks after transverse aortic constriction (TAC). Bar graphs show the interstitial fibrotic area (%) in the left ventricles (LVs) of *Bsg*^{+/-} and *Bsg*^{+/+} mice after TAC or sham operation (n=8 in each group). Scale bars, 200 μ m. **B**, Representative immunostaining of the LV at 4 weeks after SHAM or TAC in *Bsg*^{+/-} and *Bsg*^{+/+} mice. Scale bars, 200 μ m. **C**, Relative mRNA expressions of fibrotic markers, such as collagen 1a (Col1a) and connective tissue growth factor (CTGF), Bsg, and brain natriuretic peptide (BNP) in the LV of *Bsg*^{+/-} and *Bsg*^{+/+} mice at 1 week after TAC or SHAM (n=5–8). **D**, Relative mRNA expressions of interleukin-6 (IL-6), IL-1 β , and tumor necrosis factor- α (TNF- α) in the LV of *Bsg*^{+/-} and *Bsg*^{+/+} mice (n=5–8) at 1 week after TAC or SHAM. Results are expressed as mean \pm SEM. CyPA indicates cyclophilin A; and α SMA, α -smooth muscle actin. **P*<0.05.

Consistent with these findings, *Bsg*^{+/-} CFs were significantly less proliferative compared with *Bsg*^{+/+} CFs (Figure 5D). Because Bsg knockdown significantly reduced the secretion of cytokines/chemokines and growth factors from CFs (Figure 4; Figures VI and VII in the online-only Data Supplement), we compared the proliferation of CFs by treatment with conditioned medium. Cell proliferation was significantly promoted by the treatment with conditioned medium, especially by that from *Bsg*^{+/+} CFs (Figure 5E). We further performed Western blotting of conditioned medium to evaluate the secretion of Col1a and Col3a from CFs by Ang II treatment for 24 hours. The secretion of Col1a and Col3a was significantly reduced in *Bsg*^{+/-} CFs compared with *Bsg*^{+/+} CFs (Figure VIII in the online-only Data Supplement). These findings suggest that both cell surface Bsg and extracellular soluble form of Bsg promote CF proliferation and activate cardiomyocytes in response to hypertrophic stimulus.

Although these data demonstrated that Bsg in CFs plays a crucial role in the development of inflammation and heart failure, the responsive Bsg upregulation was especially strong in the cell membrane of cardiomyocytes (Figure 2A; Figure II in the online-only Data Supplement). Here, to

further examine the role of Bsg in cardiomyocytes, we performed TAC in cardiomyocyte-specific Bsg-overexpressing mice (*Bsg*-Tg). *Bsg*-Tg mice showed significantly high-Bsg expression in cardiomyocytes (Figure IXA and IXB in the online-only Data Supplement). Importantly, *Bsg*-Tg mice showed significantly poor survival compared with littermate controls after TAC (Figure 5F). Consistently, echocardiography showed significantly reduced cardiac function in *Bsg*-Tg mice compared with control mice after TAC in a time-dependent manner (Figure IXC in the online-only Data Supplement). We further evaluated the proliferation of CFs in *Bsg*-overexpressing mice in vivo. Interestingly, Elastica–Masson staining of hearts demonstrated that the interstitial fibrotic area in the LVs was significantly increased in cardiomyocyte-specific overexpressing mice (*Bsg*-Tg) compared with littermate controls after TAC (Figure 5H). Moreover, the levels of cytokines/chemokines and growth factors in heart homogenates were elevated in *Bsg*-Tg mice compared with controls (Figure X in the online-only Data Supplement), especially for interferon- γ , regulated on activation normal T cell expressed and secreted and basic-fibroblast growth factor (Figure 5G). We further performed experiments using NRCM

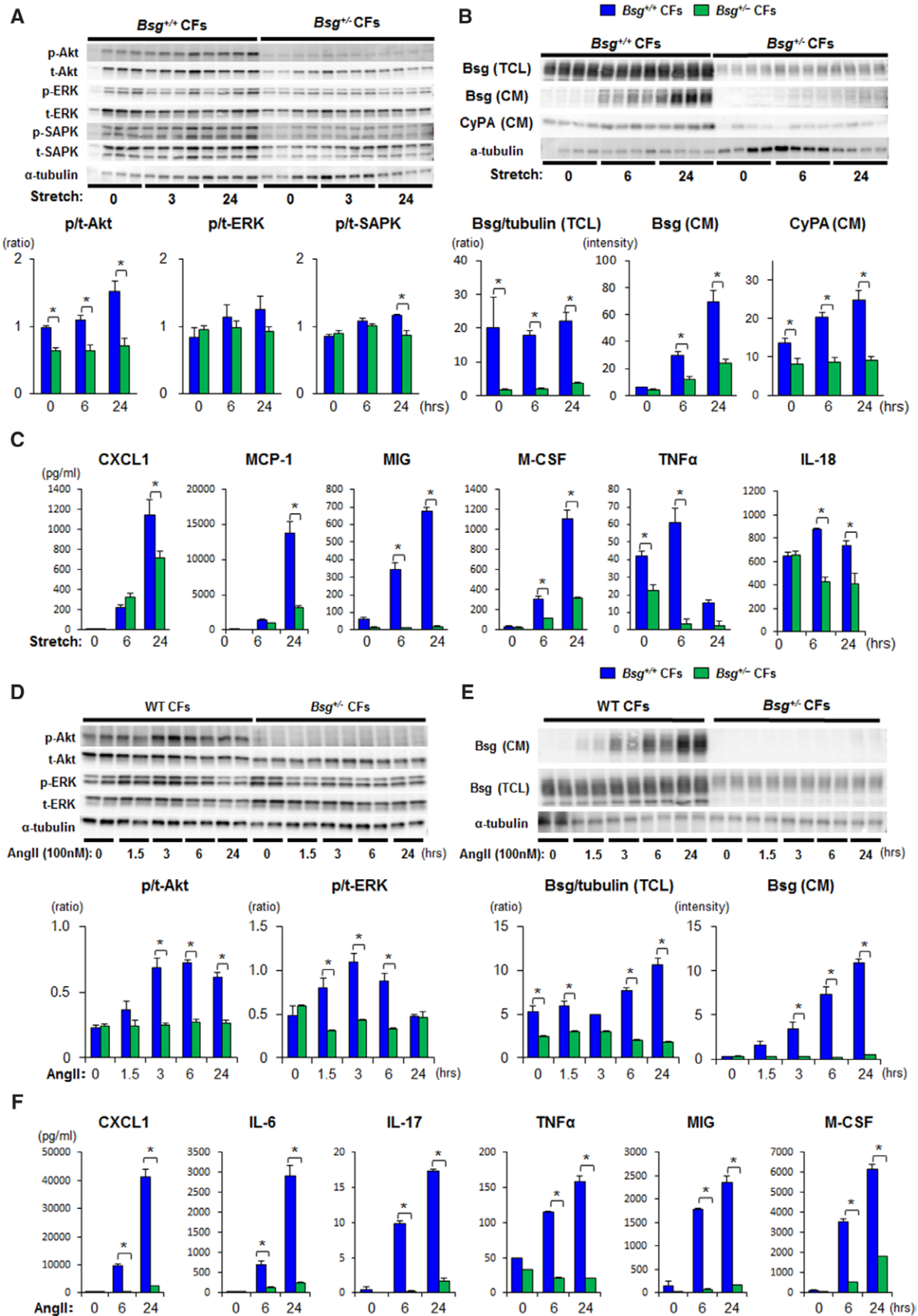


Figure 4. Basigin (Bsg) activates cardiac fibroblasts (CFs) and enhances inflammation. **A–C**, *Bsg*^{-/-} and *Bsg*^{+/+} CFs were subjected to mechanical cyclic stretch at 1 Hz with 20% elongation for 0, 6, and 24 hours (n=4 each), and then total cell lysates (TCL) and conditioned medium (CM) were collected. **A**, Quantitative Western blotting analyses of Akt, extracellular signal-regulated kinase 1/2 (ERK1/2), (Continued)

Figure 4 (Continued). and JNK activation (phosphorylated/total-Akt, ERK, and JNK) in TCL. **B**, Quantitative Western blotting analyses of Bsg in TCL and CM and cyclophilin A (CyPA) secretion in CM. **C**, Levels of cytokines/chemokines and growth factors secreted from *Bsg^{+/-}* and *Bsg^{+/+}* CFs, such as monocyte chemoattractant protein-1 (MCP-1), monokine induced by γ -interferon (MIG), tumor necrosis factor- α (TNF α), and interleukin-18 (IL-18). Results are expressed as mean \pm SEM. **P*<0.05. **D–F**, *Bsg^{+/-}* and *Bsg^{+/+}* CFs were stimulated by angiotensin II (Ang II; 100 nmol/L) for 0, 1.5, 3, 6, and 24 hours (n=3 each), and then TCL and CM were collected. **D**, Quantitative Western blotting analysis of Akt, ERK, and stress-activated protein kinase (SAPK) activation (phosphorylated/total-Akt, ERK, and SAPK) in TCL. **E**, Quantitative Western blotting analyses of Bsg expression in TCL and CM. Bsg expression and secretion were significantly less in *Bsg^{+/-}* CFs than in *Bsg^{+/+}* CFs. **F**, Levels of cytokines/chemokines and growth factors secreted from *Bsg^{+/-}* and *Bsg^{+/+}* CFs, such as IL-6, IL-17, TNF α , MIG, and macrophage colony-stimulating factor (M-CSF). Results are expressed as mean \pm SEM. **P*<0.05.

that was stimulated with recombinant Bsg or inhibited by using siRNA. Interestingly, Bsg siRNA significantly reduced NRCM survival compared with control (Figure XIA in the online-only Data Supplement). In contrast, treatment with recombinant Bsg had no effects on the survival of NRCM (Figure XIB in the online-only Data Supplement). Next, we further evaluated the paracrine effects of CF-derived Bsg

on cardiomyocytes. Here, we used the conditional medium from CF in response to cyclic stretch to stimulate NRCMs with or without an inhibitory antibody to Bsg (Bsg-Ab) for \leq 24 hours. Interestingly, treatment of NRCM with the inhibitory antibody to Bsg significantly reduced oxidative stress levels assessed by DCF staining compared with controls (Figure XIC in the online-only Data Supplement). We

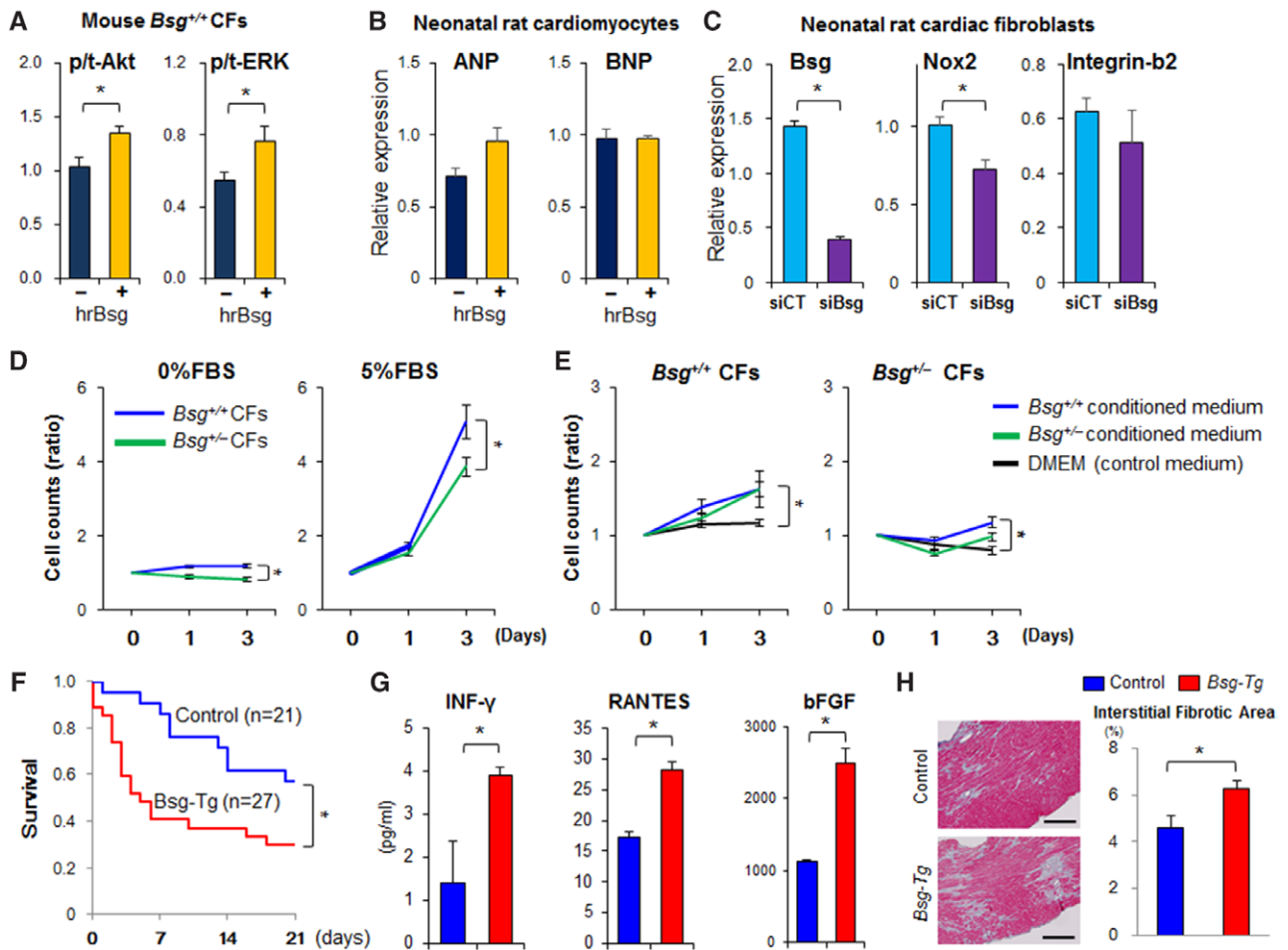


Figure 5. Basigin (Bsg) promotes cell activation and proliferation in a paracrine manner. **A**, Quantitative Western blotting analyses of Akt and extracellular signal-regulated kinase (ERK) activation (p/t-Akt and p/t-ERK) in *Bsg^{+/+}* cardiac fibroblasts (CFs) that were treated with human recombinant Bsg (hrBsg, 100 ng/mL, 1 hour; n=5 in each group). **B**, Relative mRNA expressions of hypertrophic markers, such as atrial natriuretic peptide (ANP) and brain natriuretic peptide (BNP), in neonatal rat cardiomyocytes treated with hrBsg (10 ng/mL, 1 hour; n=4 in each group). **C**, Relative mRNA expressions of Bsg, Nox2, and integrin- β 2 in neonatal rat CFs after transfection with Bsg siRNA (siBsg) or control siRNA (siCT; n=4 in each group). **D**, Proliferation assay (Cell Titer 96 MTT assay) of *Bsg^{+/-}* and *Bsg^{+/+}* CFs by treatment with Dulbecco's modified eagle medium (DMEM) with fetal bovine serum (FBS; 0% vs 5%) for 5 days (n=8 in each group). **E**, Cell proliferation of *Bsg^{+/-}* and *Bsg^{+/+}* CFs after treatment with 2% conditioned medium (CM) prepared from *Bsg^{+/-}* and *Bsg^{+/+}* CFs after 24 hours of mechanical stretch (n=8 in each group). **F**, Survival curves of cardiomyocyte-specific overexpressing mice (Bsg-Tg) and littermate controls after TAC. **G**, Levels of interferon- γ (INF- γ), regulated on activation, normal T cell expressed and secreted (RANTES) and basic-fibroblast growth factor (FGF) in the hearts from Bsg-Tg and control mice (n=3). **H**, Representative photomicrographs of Elastica-Masson staining of hearts from Bsg-Tg and control mice at 2 weeks after transverse aortic constriction (TAC). Bar graphs show the interstitial fibrotic area (%) in the left ventricle of *Bsg^{+/-}* and *Bsg^{+/+}* mice after TAC (n=4–5). Scale bars, 200 μ m. Results are expressed as mean \pm SEM. **P*<0.05.

further performed analysis of the casual link between reactive oxygen species overproduction and the Bsg-dependent cardiac phenotype. At first, NRCM was treated with Ang II with or without resveratrol, which is a popular antioxidant. Interestingly, resveratrol tended to reduce Bsg expression of NRCM in a time-dependent manner (Figure XIX in the online-only Data Supplement). Next, we stimulated NRCM with recombinant Bsg to evaluate the expression of Nox enzymes. Interestingly, recombinant Bsg significantly upregulated Nox2 expression, but not Nox4 expression, in NRCM (Figure XIE in the online-only Data Supplement). These data suggest that cell surface Bsg in cardiomyocytes augments the development of inflammation and pressure overload-induced cardiac hypertrophy and failure.

Serum Levels of sBsg Predict Prognosis in Patients With Heart Failure

Because we found that Bsg plays a crucial role in pressure overload-induced heart failure in mice, we next assessed the role of Bsg in patients with heart failure. To confirm the clinical implication of Bsg, we performed cell proliferation assay in human CFs. Treatment with hrBsg significantly increased proliferation of human CFs compared with controls (Figure 6A). In contrast, Bsg knockdown by siRNA significantly reduced proliferation of human CFs compared with control siRNA (Figure 6B). To further examine the clinical implication, we assessed serum levels of sBsg in patients with heart failure. The clinical characteristics and laboratory data of patients with heart failure are shown in Table I in the online-only Data Supplement.

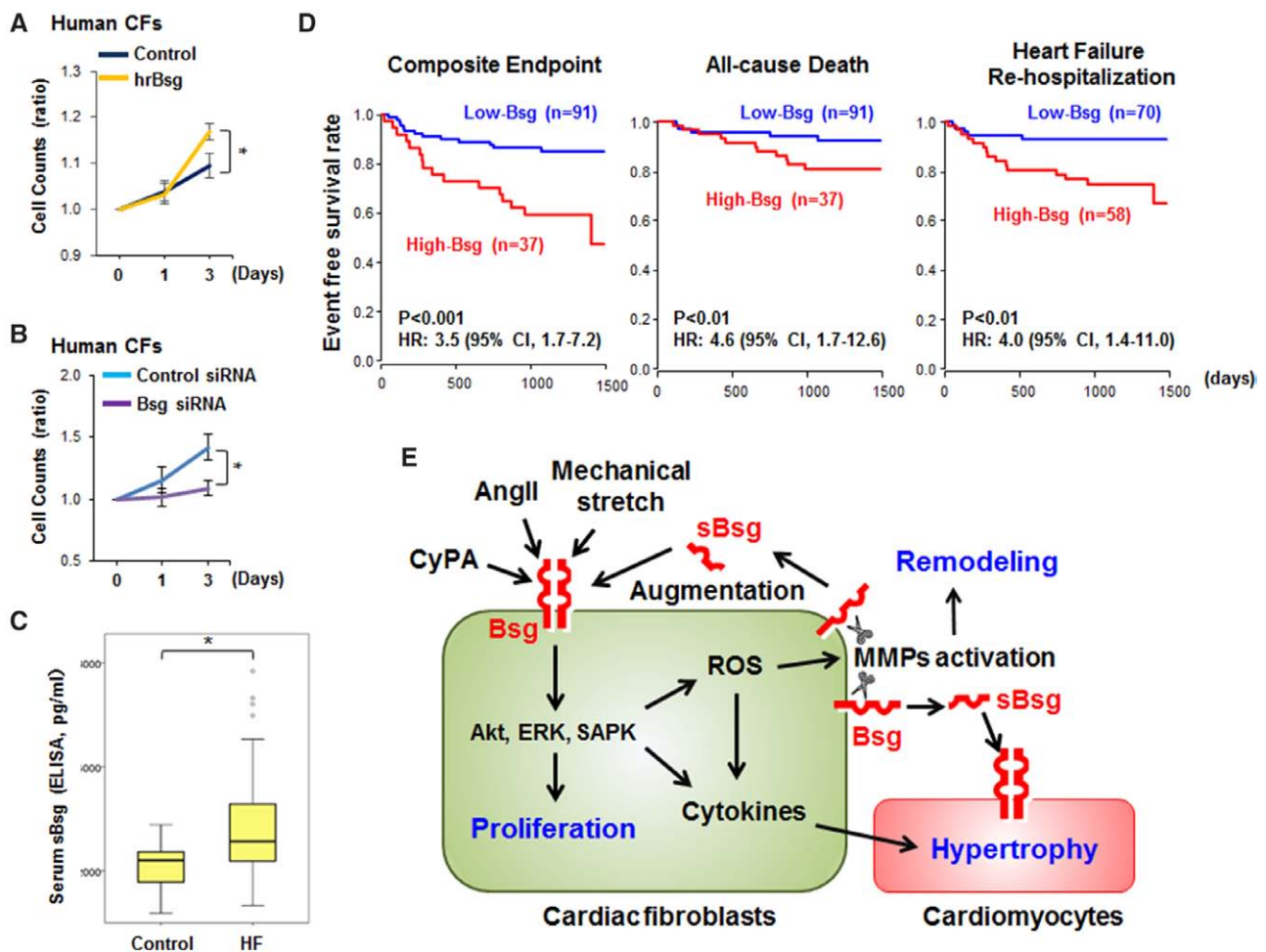


Figure 6. Serum levels of basigin (Bsg) as a novel prognostic biomarker for patients with heart failure. **A**, Cell proliferation assessed by using Cell Titer 96 MTT assay. Human cardiac fibroblasts (hCFs) were stimulated with human recombinant Bsg (hrBsg; 10 ng/mL) for ≤ 3 days ($n=8$ in each group). **B**, hCFs were transfected with human Bsg siRNA or control siRNA, and cultured for 3 days ($n=8$ in each group). **C**, Plasma levels of soluble form of Bsg (sBsg) in patients with heart failure ($n=187$) compared with healthy controls ($n=12$). Data are box-and-whisker plots of sBsg (ELISA). **D**, The Kaplan-Meier curve in patients with high-serum sBsg and those with low-serum sBsg. On the basis of the survival CART analysis, the cut-off points of high- and low-sBsg groups were set at 3099 pg/mL in the composite end point and all-cause death and 2554 pg/mL in heart failure rehospitalization. **E**, Proposed mechanism of Bsg-mediated cardiac fibrosis and hypertrophy. Cyclic stretch and angiotensin II (Ang II) promote CFs activation and proliferation, which is mediated by cell surface Bsg. Bsg signaling activates Akt, extracellular signal-regulated kinase 1/2 (ERK1/2), and stress-activated protein kinase (SAPK) in CFs and induces cell proliferation, oxidative stress, and inflammatory cytokines, resulting in metalloproteinase (MMPs) activation. Extracellular active form of MMPs cleave cell surface Bsg and release sBsg, which interacts with cell membrane Bsg again in an autocrine/paracrine manner. As a result, Bsg forms a vicious cycle to augment proliferation of CFs and inflammatory cytokines secretion. Inflammatory cytokines and sBsg released from CFs stimulate cardiomyocyte hypertrophy and promote cardiac hypertrophy in a paracrine manner. Results are expressed as mean \pm SEM. CI indicates confidence interval; HF, heart failure; HR, hazard ratio; and ROS, reactive oxygen species. * $P<0.05$.

Importantly, we found significant elevation of sBsg in patients with heart failure compared with healthy controls (Figure 6C). Moreover, the elevation of sBsg was severe especially in patients with pressure-overloaded heart disease, such as aortic stenosis and hypertensive heart disease (Figure X11A in the online-only Data Supplement). Finally, the event-free survival curve demonstrated that high-sBsg levels were associated with poor prognosis in each end point (composite, all-cause death, and hospitalization for worsening heart failure) in patients with heart failure (Figure 6D). These data suggest that Bsg is involved in the pathogenesis of cardiac hypertrophy and heart failure and could be a novel therapeutic target and biomarker for pressure overload-induced cardiac hypertrophy and failure.

Discussion

The major findings of this study are that (1) Bsg is upregulated in pressure-overloaded heart and augments inflammation, MMPs, and oxidative stress; (2) Bsg promotes pressure overload-induced cardiac fibrosis, hypertrophy, and failure; (3) Bsg in cardiac tissue, but not in inflammatory cells, plays a dominant role for the progression of heart failure; (4) Bsg mediates mechanical stretch- and Ang II-induced activation of CFs and inflammatory cytokines secretion; (5) cell surface Bsg is cleaved and released from CFs and the free sBsg promotes cell proliferation in an autocrine/paracrine manner; (6) serum levels of sBsg are elevated in patients with heart failure and predict their prognosis. On the basis of these findings, we propose that mechanical and neurohumoral stress induce growth-promoting inflammatory responses in cardiac tissue through cell surface and extracellular Bsg with a vicious cycle formation, which could be a novel mechanism for pressure overload-induced cardiac hypertrophy and failure (Figure 6E).

Bsg in Cardiac Tissues Promotes Hypertrophy, Fibrosis, and Heart Failure

It has been reported that Bsg is highly expressed in the LV of patients with dilated cardiomyopathy, myocardial infarction, and inflammatory cardiomyopathy.^{27–29} However, the role of Bsg and its signaling in heart failure have been elusive. In this study, we precisely characterized the role of Bsg in pressure-overloaded heart and its basal mechanisms. Cardiac hypertrophy, fibrosis, and inflammation are initially adaptive responses to afterload for maintaining cardiac output.^{4,30,31} In contrast, excessive cardiac hypertrophy and fibrosis can be a risk factor for sudden cardiac death, poor prognosis, and heart failure hospitalization.^{3,32} Thus, we need to develop a novel therapeutic option for targeting the hypertrophic signaling.^{31,33,34} In this study, we demonstrated that Bsg is a novel signaling that promotes cardiac hypertrophy, fibrosis, and heart failure in response to pressure overload. These responses were accompanied by significant upregulation of inflammatory cytokines/chemokines and growth factors by Bsg in CFs and cardiomyocytes. Notably, survival rate of mice was significantly improved by Bsg knockdown and worsened by cardiomyocyte-specific Bsg overexpression. It has already been demonstrated that cardiac-specific Bsg-overexpressing mice (Bsg-Tg) show myocardial remodeling and dysfunction in aging mice.³⁵ Consistent with this report, Bsg-Tg mice showed reduced LV systolic function

at baseline and especially after TAC. Moreover, in this study, we demonstrated severe cardiac fibrosis in Bsg-Tg mice after TAC, which is consistent with the previous report that showed increased fibrosis in old Bsg-Tg mice compared with younger mice.³⁵ In addition, it has been reported that cardiomyocyte-derived Bsg induces MMPs expressions and activities by oxidative stress and β -adrenergic stimuli.³⁶ These findings indicate important role of cardiomyocyte-derived Bsg in the development of pressure overload-induced cardiac fibrosis and failure. It is important to elucidate the role of BM-derived Bsg for the development of cardiac hypertrophy and fibrosis. Indeed, it has been reported that Bsg is highly expressed in erythroid cells and white blood cells.³⁷ However, in this study, immunostaining demonstrated that Bsg expression in green fluorescent protein-positive BM-derived cells was relatively weak compared with that of cardiomyocytes. Thus, we have focused on the role of Bsg in cardiac tissues and used cardiomyocyte-specific Bsg-overexpressing mice. However, further analysis of the role of BM-derived Bsg will provide us important information about the Bsg-mediated inflammation and cardiac fibrosis. Bsg is also called extracellular MMP inducer (EMMPRIN), which indicates an inducer of several kinds of MMPs,³⁸ and thus potently promotes cardiac remodeling. In this study, TAC upregulated Bsg expression and MMP activities in loaded LV in a time-dependent manner. However, the extent of which was cancelled by Bsg knockdown in mice, suggesting that Bsg plays a crucial role for TAC-induced MMP activation and cardiac remodeling. Thus, inhibition of Bsg signaling could be a novel therapeutic target for heart failure.

Inflammatory Response of CFs to Pressure Overload

It is known that CFs promote cardiac hypertrophy, dysfunction, and inflammation.^{39–41} CFs produce a variety of cytokines, such as IL-6, endothelin-1, and insulin-like growth factor-1, all of which induce hypertrophic response in cardiomyocytes in a paracrine manner.^{40,42,43} In this study, we demonstrated that cell surface Bsg is cleaved and secreted from CFs in response to stimulus by mechanical stretch and Ang II. Moreover, treatment with hrBsg activated mitogen-activated protein kinase in CFs and promoted cell proliferation. In addition, hrBsg upregulated atrial natriuretic peptide expression in cardiomyocytes. Interestingly, mechanical stretch-mediated secretion of inflammatory cytokines/chemokines and growth factors was also downregulated by Bsg knockdown in CFs, which implicates the role of Bsg as a mechanotransducer in cardiac tissues. These data indicate that sBsg secreted from CFs affects CFs themselves and cardiomyocytes in an autocrine/paracrine manner. Thus, both cell surface Bsg and soluble form of Bsg could be a novel therapeutic target for attenuating cardiac hypertrophy, fibrosis, and failure.

Bsg as a Therapeutic Target and a Novel Biomarker

When we consider Bsg as a novel therapeutic target, there are several compounds for Bsg inhibition. For direct inhibition, there are several reports that demonstrated the role of Bsg monoclonal antibodies to ameliorate atherosclerosis, myocardial infarction, and cancers in mice.^{27,44,45} For indirect inhibition, berberine, resveratrol, and curcumin have been reported to inhibit

Bsg expression through regulation of mitogen-activated protein kinase and reactive oxygen species.^{46–49} In this study, we showed that systemic Bsg inhibition showed resistance to chronic pressure overload in mice *in vivo*. Thus, inhibition of Bsg could be a promising therapeutic strategy for heart failure.

Next, this study provides novel evidence that serum levels of sBsg are increased in patients with heart failure. In addition, higher sBsg levels predicted all-cause death and heart failure hospitalization. It has been reported that serum levels of sBsg are increased in patients with hepatocellular carcinoma, lupus nephritis, and systemic sclerosis.^{21,50,51} Moreover, in this study, serum sBsg levels had strong correlations with serum IL-8, monokine induced by γ -interferon, adiponectin, and CyPA, indicating the inflammatory role of Bsg in humans. It has been reported that high levels of serum IL-8 and adiponectin predict poor prognosis in patients with heart failure,^{52,53} which also supports our findings that serum sBsg levels could be a promising biomarker for patients with heart failure. Further study will provide additional knowledge as to the usefulness of sBsg in patients with heart failure.

In conclusions, we were able to demonstrate that Bsg in cardiac tissue plays a crucial role in pressure overload-induced heart failure in mice and patients with heart failure. Bsg could be a novel therapeutic target and a biomarker for heart failure.

Acknowledgments

We are grateful to the laboratory members in the Department of Cardiovascular Medicine of Tohoku University Graduate School of Medicine for valuable technical assistance, especially Hiromi Yamashita, Ai Nishihara, and Yumi Watanabe.

Sources of Funding

This work was supported, in part, by the Takeda Science Foundation, the grant-in-aid for Tohoku University Global COE for Conquest of Signal Transduction Diseases with Network Medicine and the grants-in-aid for Scientific Research (21790698, 23659408, 24390193, 15H02535, 15H04816, and 15K15046), all of which are from the Ministry of Education, Culture, Sports, Science, and Technology, Tokyo, Japan, and the grants-in-aid for Scientific Research from the Ministry of Health, Labour, and Welfare, Tokyo, Japan (10102895 and 15545346).

Disclosures

None.

References

- Roger VL. Epidemiology of heart failure. *Circ Res*. 2013;113:646–659.
- Sharma K, Kass DA. Heart failure with preserved ejection fraction: mechanisms, clinical features, and therapies. *Circ Res*. 2014;115:79–96. doi: 10.1161/CIRCRESAHA.115.302922.
- Oka T, Akazawa H, Naito AT, Komuro I. Angiogenesis and cardiac hypertrophy: maintenance of cardiac function and causative roles in heart failure. *Circ Res*. 2014;114:565–571. doi: 10.1161/CIRCRESAHA.114.300507.
- Lyon RC, Zanella F, Omens JH, Sheikh F. Mechanotransduction in cardiac hypertrophy and failure. *Circ Res*. 2015;116:1462–1476. doi: 10.1161/CIRCRESAHA.116.304937.
- Heineke J, Molkenin JD. Regulation of cardiac hypertrophy by intracellular signalling pathways. *Nat Rev Mol Cell Biol*. 2006;7:589–600. doi: 10.1038/nrm1983.
- Takimoto E, Kass DA. Role of oxidative stress in cardiac hypertrophy and remodeling. *Hypertension*. 2007;49:241–248. doi: 10.1161/01.HYP.0000254415.31362.a7.
- Sugden PH. Ras, Akt, and mechanotransduction in the cardiac myocyte. *Circ Res*. 2003;93:1179–1192. doi: 10.1161/01.RES.0000106132.04301.F5.
- Molkenin JD. Calcineurin and beyond: cardiac hypertrophic signaling. *Circ Res*. 2000;87:731–738.
- Ikeda S, Satoh K, Kikuchi N, Miyata S, Suzuki K, Omura J, Shimizu T, Kobayashi K, Kobayashi K, Fukumoto Y, Sakata Y, Shimokawa H. Crucial role of rho-kinase in pressure overload-induced right ventricular hypertrophy and dysfunction in mice. *Arterioscler Thromb Vasc Biol*. 2014;34:1260–1271. doi: 10.1161/ATVBAHA.114.303320.
- Satoh K, Nigro P, Zeidan A, Soe NN, Jaffré F, Oikawa M, O'Dell MR, Cui Z, Menon P, Lu Y, Mohan A, Yan C, Blaxall BC, Berk BC. Cyclophilin A promotes cardiac hypertrophy in apolipoprotein E-deficient mice. *Arterioscler Thromb Vasc Biol*. 2011;31:1116–1123. doi: 10.1161/ATVBAHA.110.214601.
- Asaumi Y, Kagaya Y, Takeda M, Yamaguchi N, Tada H, Ito K, Ohta J, Shirato T, Shirato K, Minegishi N, Shimokawa H. Protective role of endogenous erythropoietin system in nonhematopoietic cells against pressure overload-induced left ventricular dysfunction in mice. *Circulation*. 2007;115:2022–2032. doi: 10.1161/CIRCULATIONAHA.106.659037.
- Iacono KT, Brown AL, Greene MI, Saouaf SJ. CD147 immunoglobulin superfamily receptor function and role in pathology. *Exp Mol Pathol*. 2007;83:283–295. doi: 10.1016/j.yexmp.2007.08.014.
- Huet E, Vallée B, Szul D, Verrecchia F, Mourah S, Jester JV, Hoang-Xuan T, Menashi S, Gabison EE. Extracellular matrix metalloproteinase inducer/CD147 promotes myofibroblast differentiation by inducing alpha-smooth muscle actin expression and collagen gel contraction: implications in tissue remodeling. *FASEB J*. 2008;22:1144–1154. doi: 10.1096/fj.07-8748com.
- Gou X, Ru Q, Zhang H, Chen Y, Li L, Yang H, Xing J, Chen Z. HAb18G/CD147 inhibits starvation-induced autophagy in human hepatoma cell SMMC7721 with an involvement of Beclin 1 down-regulation. *Cancer Sci*. 2009;100:837–843. doi: 10.1111/j.1349-7006.2009.01113.x.
- Satoh K, Satoh T, Kikuchi N, et al. Basigin mediates pulmonary hypertension by promoting inflammation and vascular smooth muscle cell proliferation. *Circ Res*. 2014;115:738–750. doi: 10.1161/CIRCRESAHA.115.304563.
- Seizer P, Ungern-Sternberg SN, Schönberger T, Borst O, Münzer P, Schmidt EM, Mack AF, Heinzmann D, Chatterjee M, Langer H, Malešević M, Lang F, Gawaz M, Fischer G, May AE. Extracellular cyclophilin A activates platelets via EMMPRIN (CD147) and PI3K/Akt signaling, which promotes platelet adhesion and thrombus formation *in vitro* and *in vivo*. *Arterioscler Thromb Vasc Biol*. 2015;35:655–663. doi: 10.1161/ATVBAHA.114.305112.
- Crosnier C, Bustamante LY, Bartholdson SJ, Bei AK, Theron M, Uchikawa M, Mboup S, Ndir O, Kwiatkowski DP, Duraisingh MT, Rayner JC, Wright GJ. Basigin is a receptor essential for erythrocyte invasion by *Plasmodium falciparum*. *Nature*. 2011;480:534–537. doi: 10.1038/nature10606.
- Tang W, Chang SB, Hemler ME. Links between CD147 function, glycosylation, and caveolin-1. *Mol Biol Cell*. 2004;15:4043–4050. doi: 10.1091/mbc.E04-05-0402.
- Agrawal SM, Yong VW. The many faces of EMMPRIN - roles in neuroinflammation. *Biochim Biophys Acta*. 2011;1812:213–219. doi: 10.1016/j.bbdis.2010.07.018.
- Yan L, Zucker S, Toole BP. Roles of the multifunctional glycoprotein, emmprin (basigin; CD147), in tumour progression. *Thromb Haemost*. 2005;93:199–204. doi: 10.1160/TH04-08-0536.
- Maeda-Hori M, Kosugi T, Kojima H, et al. Plasma CD147 reflects histological features in patients with lupus nephritis. *Lupus*. 2014;23:342–352. doi: 10.1177/0961203314520840.
- Damsker JM, Okwumabua I, Pushkarsky T, Arora K, Bukrinsky MI, Constant SL. Targeting the chemotactic function of CD147 reduces collagen-induced arthritis. *Immunology*. 2009;126:55–62. doi: 10.1111/j.1365-2567.2008.02877.x.
- Schmidt R, Bültmann A, Fischel S, Gillitzer A, Cullen P, Walch A, Jost P, Ungerer M, Tolley ND, Lindemann S, Gawaz M, Schömig A, May AE. Extracellular matrix metalloproteinase inducer (CD147) is a novel receptor on platelets, activates platelets, and augments nuclear factor kappaB-dependent inflammation in monocytes. *Circ Res*. 2008;102:302–309. doi: 10.1161/CIRCRESAHA.107.157990.
- Haug C, Lenz C, Díaz F, Bachem MG. Oxidized low-density lipoproteins stimulate extracellular matrix metalloproteinase inducer (EMMPRIN) release by coronary smooth muscle cells. *Arterioscler Thromb Vasc Biol*. 2004;24:1823–1829. doi: 10.1161/01.ATV.0000142806.59283.11.
- Lizarbe TR, Tarín C, Gómez M, Lavin B, Aracil E, Orte LM, Zaragoza C. Nitric oxide induces the progression of abdominal aortic aneurysms through the matrix metalloproteinase inducer EMMPRIN. *Am J Pathol*. 2009;175:1421–1430. doi: 10.2353/ajpath.2009.080845.

26. Miller LH, Ackerman HC, Su XZ, Wellems TE. Malaria biology and disease pathogenesis: insights for new treatments. *Nat Med*. 2013;19:156–167. doi: 10.1038/nm.3073.
27. Seizer P, Oehmann C, Schönberger T, Zach S, Rose M, Borst O, Klingel K, Kandolf R, MacDonald HR, Nowak RA, Engelhardt S, Lang F, Gawaz M, May AE. Disrupting the EMMPRIN (CD147)-cyclophilin A interaction reduces infarct size and preserves systolic function after myocardial ischemia and reperfusion. *Arterioscler Thromb Vasc Biol*. 2011;31:1377–1386. doi: 10.1161/ATVBAHA.111.225771.
28. Spinale FG, Coker ML, Heung LJ, Bond BR, Gunasinghe HR, Etoh T, Goldberg AT, Zellner JL, Crumbley AJ. A matrix metalloproteinase induction/activation system exists in the human left ventricular myocardium and is upregulated in heart failure. *Circulation*. 2000;102:1944–1949.
29. Seizer P, Geisler T, Bigalke B, Schneider M, Klingel K, Kandolf R, Stellos K, Schrieck J, Gawaz M, May AE. EMMPRIN and its ligand cyclophilin A as novel diagnostic markers in inflammatory cardiomyopathy. *Int J Cardiol*. 2013;163:299–304. doi: 10.1016/j.ijcard.2011.06.049.
30. Higashikuni Y, Tanaka K, Kato M, Nureki O, Hirata Y, Nagai R, Komuro I, Sata M. Toll-like receptor-2 mediates adaptive cardiac hypertrophy in response to pressure overload through interleukin-1 β upregulation via nuclear factor κ B activation. *J Am Heart Assoc*. 2013;2:e000267. doi: 10.1161/JAHA.113.000267.
31. Baudino TA, Carver W, Giles W, Borg TK. Cardiac fibroblasts: friend or foe? *Am J Physiol Heart Circ Physiol*. 2006;291:H1015–H1026. doi: 10.1152/ajpheart.00023.2006.
32. Gulati A, Jabbour A, Ismail TF, et al. Association of fibrosis with mortality and sudden cardiac death in patients with nonischemic dilated cardiomyopathy. *JAMA*. 2013;309:896–908. doi: 10.1001/jama.2013.1363.
33. Schiattarella GG, Hill JA. Inhibition of hypertrophy is a good therapeutic strategy in ventricular pressure overload. *Circulation*. 2015;131:1435–1447. doi: 10.1161/CIRCULATIONAHA.115.013894.
34. Laroumanie F, Douin-Echinard V, Pozzo J, Lairez O, Tortosa F, Vinel C, Delage C, Calise D, Dutaur M, Parini A, Pizzinat N. CD4+ T cells promote the transition from hypertrophy to heart failure during chronic pressure overload. *Circulation*. 2014;129:2111–2124. doi: 10.1161/CIRCULATIONAHA.113.007101.
35. Zavadzkas JA, Plyler RA, Bouges S, Koval CN, Rivers WT, Beck CU, Chang EI, Stroud RE, Mukherjee R, Spinale FG. Cardiac-restricted overexpression of extracellular matrix metalloproteinase inducer causes myocardial remodeling and dysfunction in aging mice. *Am J Physiol Heart Circ Physiol*. 2008;295:H1394–H1402. doi: 10.1152/ajpheart.00346.2008.
36. Siwik DA, Kuster GM, Brahmabhatt JV, Zaidi Z, Malik J, Ooi H, Ghorayeb G. EMMPRIN mediates beta-adrenergic receptor-stimulated matrix metalloproteinase activity in cardiac myocytes. *J Mol Cell Cardiol*. 2008;44:210–217. doi: 10.1016/j.yjmcc.2007.07.054.
37. Su AI, Wiltshire T, Batalov S, Lapp H, Ching KA, Block D, Zhang J, Soden R, Hayakawa M, Kreiman G, Cooke MP, Walker JR, Hogenesch JB. A gene atlas of the mouse and human protein-encoding transcriptomes. *Proc Natl Acad Sci U S A*. 2004;101:6062–6067. doi: 10.1073/pnas.0400782101.
38. Nabeshima K, Iwasaki H, Koga K, Hojo H, Suzumiya J, Kikuchi M. Emmprin (basigin/CD147): matrix metalloproteinase modulator and multifunctional cell recognition molecule that plays a critical role in cancer progression. *Pathol Int*. 2006;56:359–367. doi: 10.1111/j.1440-1827.2006.01972.x.
39. Chen W, Frangiannakis NG. Fibroblasts in post-infarction inflammation and cardiac repair. *Biochim Biophys Acta*. 2013;1833:945–953. doi: 10.1016/j.bbamcr.2012.08.023.
40. Takeda N, Manabe I, Uchino Y, Eguchi K, Matsumoto S, Nishimura S, Shindo T, Sano M, Otsu K, Snider P, Conway SJ, Nagai R. Cardiac fibroblasts are essential for the adaptive response of the murine heart to pressure overload. *J Clin Invest*. 2010;120:254–265. doi: 10.1172/JCI40295.
41. Thum T, Gross C, Fiedler J, et al. MicroRNA-21 contributes to myocardial disease by stimulating MAP kinase signalling in fibroblasts. *Nature*. 2008;456:980–984. doi: 10.1038/nature07511.
42. Kaushik DK, Hahn JN, Yong VW. EMMPRIN, an upstream regulator of MMPs, in CNS biology. *Matrix Biol*. 2015;44-46:138–146. doi: 10.1016/j.matbio.2015.01.018.
43. Sangboonruang S, Thammasit P, Intasai N, Kasinrerker W, Tayapiwatana C, Tragoolpua K. EMMPRIN reduction via scFv-M6-1B9 intrabody affects α 3 β 1-integrin and MCT1 functions and results in suppression of progressive phenotype in the colorectal cancer cell line Caco-2. *Cancer Gene Ther*. 2014;21:246–255. doi: 10.1038/cgt.2014.24.
44. Dean NR, Newman JR, Helman EE, Zhang W, Safavy S, Weeks DM, Cunningham M, Snyder LA, Tang Y, Yan L, McNally LR, Buchsbaum DJ, Rosenthal EL. Anti-EMMPRIN monoclonal antibody as a novel agent for therapy of head and neck cancer. *Clin Cancer Res*. 2009;15:4058–4065. doi: 10.1158/1078-0432.CCR-09-0212.
45. Liu H, Yang LX, Guo RW, Zhu GF, Shi YK, Wang XM, Qi F, Guo CM, Ye JS, Yang ZH, Liang X. Functional blockage of EMMPRIN ameliorates atherosclerosis in apolipoprotein E-deficient mice. *Int J Cardiol*. 2013;168:3248–3253. doi: 10.1016/j.ijcard.2013.04.141.
46. Cao J, Han Z, Tian L, Chen K, Fan Y, Ye B, Huang W, Wang C, Huang Z. Curcumin inhibits EMMPRIN and MMP-9 expression through AMPK-MAPK and PKC signaling in PMA induced macrophages. *J Transl Med*. 2014;12:266. doi: 10.1186/s12967-014-0266-2.
47. Huang Z, Wang L, Meng S, Wang Y, Chen T, Wang C. Berberine reduces both MMP-9 and EMMPRIN expression through prevention of p38 pathway activation in PMA-induced macrophages. *Int J Cardiol*. 2011;146:153–158. doi: 10.1016/j.ijcard.2009.06.023.
48. Venkatesan B, Valente AJ, Reddy VS, Siwik DA, Chandrasekar B. Resveratrol blocks interleukin-18-EMMPRIN cross-regulation and smooth muscle cell migration. *Am J Physiol Heart Circ Physiol*. 2009;297:H874–H886. doi: 10.1152/ajpheart.00311.2009.
49. Huang Z, Wang C, Wei L, Wang J, Fan Y, Wang L, Wang Y, Chen T. Resveratrol inhibits EMMPRIN expression via P38 and ERK1/2 pathways in PMA-induced THP-1 cells. *Biochem Biophys Res Commun*. 2008;374:517–521. doi: 10.1016/j.bbrc.2008.07.058.
50. Yanaba K, Asano Y, Tada Y, Sugaya M, Kadono T, Hamaguchi Y, Sato S. Increased serum soluble CD147 levels in patients with systemic sclerosis: association with scleroderma renal crisis. *Clin Rheumatol*. 2012;31:835–839. doi: 10.1007/s10067-012-1949-9.
51. Moonsom S, Tayapiwatana C, Wongkham S, Kongtawelert P, Kasinrerker W. A Competitive ELISA for quantifying serum CD147: reduction of soluble CD147 levels in cancer patient sera. *Hybridoma (Larchmt)*. 2010;29:45–52. doi: 10.1089/hyb.2009.0096.
52. Nymo SH, Hulthe J, Ueland T, McMurray J, Wikstrand J, Askevold ET, Yndestad A, Gullestad L, Aukrust P. Inflammatory cytokines in chronic heart failure: interleukin-8 is associated with adverse outcome. Results from CORONA. *Eur J Heart Fail*. 2014;16:68–75. doi: 10.1093/eurjhf/hft125.
53. Kistorp C, Faber J, Galatius S, Gustafsson F, Frystyk J, Flyvbjerg A, Hildebrandt P. Plasma adiponectin, body mass index, and mortality in patients with chronic heart failure. *Circulation*. 2005;112:1756–1762. doi: 10.1161/CIRCULATIONAHA.104.530972.

Significance

Heart failure is a major cause of death and mortality rate still remains high, but fundamental therapies have not been developed yet. Bsg was reported to be upregulated in LV in patients with heart failure; however, the role of Bsg in heart failure remains to be elucidated. In this study, we showed that Bsg deletion improved pressure overload–induced cardiac hypertrophy, fibrosis, and failure in mice through inhibition of MMPs, inflammation, and oxidative stress. Furthermore, we showed that extracellular and intracellular Bsg promoted CFs proliferation and make a vicious cycle to augment cardiac fibrosis in an autocrine and paracrine manner. Furthermore, serum levels of sBsg in patients with heart failure were markedly upregulated and predicted poor prognosis in patients with heart failure. These results provided the evidence that Bsg could be a novel therapeutic target and serum sBsg could be a potential prognostic biomarker for patients with heart failure.

Arteriosclerosis, Thrombosis, and Vascular Biology



JOURNAL OF THE AMERICAN HEART ASSOCIATION

Basigin Promotes Cardiac Fibrosis and Failure in Response to Chronic Pressure Overload in Mice

Kota Suzuki, Kimio Satoh, Shohei Ikeda, Shinichiro Sunamura, Tomohiro Otsuki, Taijyu Satoh, Nobuhiro Kikuchi, Junichi Omura, Ryo Kurosawa, Masamichi Nogi, Kazuhiko Numano, Koichiro Sugimura, Tatsuo Aoki, Shunsuke Tatebe, Satoshi Miyata, Rupak Mukherjee, Francis G. Spinale, Kenji Kadomatsu and Hiroaki Shimokawa

Arterioscler Thromb Vasc Biol. 2016;36:636-646; originally published online February 25, 2016;

doi: 10.1161/ATVBAHA.115.306686

Arteriosclerosis, Thrombosis, and Vascular Biology is published by the American Heart Association, 7272 Greenville Avenue, Dallas, TX 75231

Copyright © 2016 American Heart Association, Inc. All rights reserved.

Print ISSN: 1079-5642. Online ISSN: 1524-4636

The online version of this article, along with updated information and services, is located on the World Wide Web at:

<http://atvb.ahajournals.org/content/36/4/636>

Permissions: Requests for permissions to reproduce figures, tables, or portions of articles originally published in *Arteriosclerosis, Thrombosis, and Vascular Biology* can be obtained via RightsLink, a service of the Copyright Clearance Center, not the Editorial Office. Once the online version of the published article for which permission is being requested is located, click Request Permissions in the middle column of the Web page under Services. Further information about this process is available in the [Permissions and Rights Question and Answer](#) document.

Reprints: Information about reprints can be found online at:
<http://www.lww.com/reprints>

Subscriptions: Information about subscribing to *Arteriosclerosis, Thrombosis, and Vascular Biology* is online at:
<http://atvb.ahajournals.org/subscriptions/>

Permissions: Requests for permissions to reproduce figures, tables, or portions of articles originally published in *Arteriosclerosis, Thrombosis, and Vascular Biology* can be obtained via RightsLink, a service of the Copyright Clearance Center, not the Editorial Office. Once the online version of the published article for which permission is being requested is located, click Request Permissions in the middle column of the Web page under Services. Further information about this process is available in the [Permissions and Rights Question and Answer](#) document.

Reprints: Information about reprints can be found online at:
<http://www.lww.com/reprints>

Subscriptions: Information about subscribing to *Arteriosclerosis, Thrombosis, and Vascular Biology* is online at:
<http://atvb.ahajournals.org//subscriptions/>

SUPPLEMENTAL MATERIAL

Supplemental Methods

Animal Experiments

All animal experiments were conducted in accordance with the protocols approved by the Tohoku University Animal Care and Use Committee. Pressure overload-induced heart failure models were used to assess the role of Bsg on heart failure development in mice. Body weight between 23 and 30 g male Bsg deficient (*Bsg*^{+/-}) mice and cardiomyocytes-specific Bsg overexpressing (Bsg-Tg) mice and their littermate controls on a normal chow diet were exposed to severe pressure overload by transverse aortic constriction (TAC). TAC procedures were performed as we previously reported.¹⁻³ Briefly, the animals were anesthetized with isoflurane and maintained body temperature. The transverse aorta was banded with a 6-0 suture, tied tight against a 27-gauge needle, which was removed quickly. Sham operated mice underwent the same procedure but without tying the transverse aorta. Mice with transverse aortic velocity above 4 m/s assessed by echocardiography were enrolled for the present study. The assessment of heart failure and histology were performed at 4 weeks after the operation. To determine the effect of Bsg deficiency on pressure overload-induced heart failure, we performed cardiac echocardiography and weight measurements. All the operations and analyses were performed in a blinded manner with regard to the genotype of mice.

Generation and Genotyping of *Bsg*^{+/-} and Bsg-Tg Mice

All animal experiments were conducted in accordance with the experimental protocols approved by the Institutional Animal Care and Use Committee of Tohoku University (2012 Kodo-002). *Bsg*^{+/-} mice were obtained from Dr. Kadomatsu at Nagoya University (Nagoya, Japan).⁴ Bsg is an important cell-surface molecule involved in early embryogenesis and reproduction.^{5,6} Since complete Bsg disruption (*Bsg*^{-/-}) in mice results in perinatal lethality,⁶ we used *Bsg*^{+/-} mice in the present study. Cardiomyocytes-specific Bsg overexpressing mice (Bsg-Tg) were obtained from Dr. Spinale & Mukherjee at Medical University of South Carolina in the United States.⁷ Animals were housed under a 12-hour light and 12-hour dark regimen and placed on a normal chow diet. All mice were genotyped by PCR on tail clip samples. Genotyping primers were as follows: *Bsg*, Basigin forward 5'-TGGCCTTCACGCTCTTGAGC-3' and Basigin reverse 5'-GCCTCATCTCTAAGATCACT-3' and Neo forward 5'-CAGCGTCTTGTCATTGGCGA-3' and Neo reverse 5'-GCTCTTCGTCCAGATCATCC-3'; *human Bsg*, human Basigin forward

5'-GGCCAGAAAACGGAGTTCAA-3' and human Basigin reverse
5'-GCGCTTCTCGTAGATGAAGA-3'.

Blood Pressure and Echocardiography

Blood pressure at baseline was measured by the tail-cuff system (Muromachi Kikai Co, Ltd, MK-2000ST NP-NIBP Monitor, Tokyo, Japan) without anesthesia. Echocardiography was performed using the Vevo 2100 (Visualsonics, Toronto, Canada) under inhalation of isoflurane (0.5-1.0% v/v). Echocardiography was performed to measure LV dimensions and functions at the level of papillary muscles in M-mode tracings as previously described.¹

Bone Marrow Transplantation

Bone marrow transplantation was performed as previously described.⁸⁻¹² Briefly, 8-week-old *Bsg*^{+/+} and *Bsg*^{+/-} recipient mice were lethally irradiated (9.6 Gy) and received an intravenous tail injection of 5×10^6 donor GFP⁺ bone marrow cells (*Bsg*^{+/+} or *Bsg*^{+/-}) suspended in 100 μ l calcium- and magnesium-free PBS with 2% fetal bovine serum (FBS). After bone marrow transplantation, the mice were placed on a regular chow diet for 4 weeks followed by TAC for another 4 weeks. Transgenic mice ubiquitously expressing green fluorescent protein (GFP) were obtained from the Jackson Laboratory. To obtain the chimeric mice, we crossed *Bsg*^{+/-} mice with GFP mice, and they were born in expected Mendelian ratio.

Histology

After echocardiographic measurements, animals were anesthetized with isoflurane (2.0%). For morphological analysis, mice were perfused with cold phosphate-buffered saline (PBS) and perfusion-fixed with 10% phosphate-buffered formalin at physiological pressure for 5 min. The whole heart and lungs were harvested, fixed for 24 h, embedded in paraffin and cross sections (5 μ m) were prepared. Paraffin sections were stained with hematoxylin-eosin (HE) and Elastica-Masson (for analysis of the myocardial fibrosis area) or used for immunostaining. These analyses were performed by light microscopy (BX51, Olympus, Tokyo, Japan) and Inage J Software (NIH, Bethesda, MD, USA).

Immunohistochemistry

Human heart tissues were obtained from patients with DCM at the time of heart transplantation. All patients provided written consent for the use of their heart tissues for research. Ethics approval was obtained from the Ethics Committee of Tohoku University Graduate School of

Medicine (#2013-1-230). For immunofluorescence staining, mice were anesthetized with isoflurane and perfused with cold PBS and fixed by 4% phosphate-buffered paraformaldehyde, which were embedded in OCT (Tissue-Tek; Miles Ink., Elkhart, Illinois, USA). For immunostaining, we used following primary antibodies; Bsg (1:400 dilution; R&D systems, AF972 for human tissue and AF772 for mouse tissue), CyPA polyclonal (1:1000 dilution; BIOMOL Research Laboratories, Inc.), α -smooth muscle actin (α SMA, clone 1A4, 1:400 dilution; Sigma-Aldrich, A5691), leukocyte common antigen, CD45 (clone Ly-5, 1:100 dilution; BD Pharmingen, #550539), and α -actinin (1:200 dilution; BD Pharmingen, #612576). Slides were viewed with a microscope (BX51, Olympus, Tokyo, Japan) equipped with a digital camera and analyzed by DP Controller and DP Manager Software (Olympus, Tokyo, Japan) or confocal microscopy (Zeiss, LSM780).

Dihydroethidium Staining

The whole heart was harvested, embedded in OCT, snap-frozen, and cross-sections (10 μ m) were prepared. Dihydroethidium (DHE), an oxidant fluorescent dye, was used to detect myocardial production of ROS as previously described.^{1, 13} Briefly, transverse sections were cut with a cryostat and placed on MAS-coated glass-slides (Matsunami Glass, Osaka, Japan). Then, the glass slides were incubated at 37°C for 30 min with DHE solution in phosphate-buffered saline (PBS) (2 μ mol/L) in the shade. After washing with PBS, DHE red fluorescence (585nm) images were obtained using a confocal microscopy (Zeiss, LSM780).

MMP Activity

To evaluate the MMPs activities in response to pressure overload *in vivo*, we used gelatin zymography. The whole heart was harvested 1 week after TAC and gelatinolytic activities were studied by gelatin zymography kit (Cosmo Bio, Tokyo, Japan). Briefly, the extracts of heart homogenates were electrophoresed in SDS-PAGE gels containing gelatin. Gels were washed and incubated for 24 hours at 37°C in zymography buffer, and thereafter stained with coomassie brilliant blue. Subsequently, gels were scanned and quantitative analysis of MMP-2 and pro-MMP-2 activities were performed by using Image J Software (NIH, Bethesda, MD, USA). For in situ zymography, freshly cut frozen heart sections (10 μ m) were incubated with a fluorogenic gelatin substrate (DQ gelatin, Molecular Probes) dissolved to 25 μ g/ml in zymography buffer (50 mmol/L Tris-HCL pH7.4 and 5 mmol/L CaCl₂) according to the manufacturer's protocol.¹⁰ Proteolytic activity was detected as green fluorescence (530 nm) by confocal microscopy (Zeiss, LSM780).

Harvest of Mouse Cardiac Fibroblasts

Mouse cardiac fibroblasts (CFs) were isolated from male mice. The heart tissue was enzymatically digested by collagenase type II (Worthington, NJ, USA), and then placed in a dish filled with Dulbecco's modified Eagle's medium (DMEM) containing 4.5 g/L glucose supplemented with 20% fetal bovine serum and 1x penicillin/streptomycin. Following removal of the atria, both ventricles were teased apart and pipetted into small pieces. The pellet containing cardiomyocytes was discarded and the supernatant, containing mostly cardiac fibroblasts (CFs), was centrifuged and re-suspended in medium. The CFs were plated and cultured on a 10 cm dish with DMEM with 10% fetal bovine serum at 37°C in a humidified atmosphere of 5% CO₂ and 95% air.¹³ Mouse CFs were stimulated with either angiotensin II (100 nmol/L) or human recombinant Basigin (972-EMN-050, R&D, MN, USA) after 24 hours starvation. To examine the cellular effects of mechanical stress, CFs were starved for 24 hours and then subjected to cyclic stretch with 20% elongation at 1Hz for up to 24 hours using Strex system (Strex, Osaka, Japan).^{14, 15} After the stimulus, medium and total cell lysate were collected. Briefly, soon after medium was collected, the CFs were washed with cold PBS and harvested on ice in cell lysis buffer (#9803, Cell Signaling, MA, USA) with proteinase inhibitor cocktail (P8340, Sigma), and medium was filtered to remove cell debris and concentrated 100-fold with an Amicon Ultracel-15 centrifugal filter (Millipore Corp, MA, USA) to yield concentrated conditioned medium (CM).¹⁶

Isolation of Neonatal Rat Cardiomyocytes and Cardiac Fibroblasts

The hearts from neonatal Wistar rats (Japan SLC, Shizuoka, Japan) were minced and dissociated with collagenase type II (Worthington, NJ, USA). Then, cells were incubated on 10 cm dishes for 30 min at 37°C in 5% CO₂ incubator. To obtain neonatal cardiomyocytes (NRCM), non-attached viable cells in supernatant were collected and supplemented with 10 μM cytosine β-d-arabinofuranoside (Sigma-Aldrich, Tokyo, Japan) to prevent growth of non-myocytes.¹⁷ To obtain neonatal cardiac fibroblasts (NRCF), attached cells to dishes were passaged and cultured in DMEM with 10% FBS. After 24 hours starvation, NRCM were treated with human recombinant Basigin for 24 hours to obtain mRNA samples. NRCM was also treated with AngII with or without resveratrol (CAS 501-36-0, Calbiochem) for up to 24 hours, thereafter Bsg gene expression was studied. NRCF were transfected with Basigin siRNA (10 nmol/l) or control siRNA (10 nmol/L) (QIAGEN, Germany) for 72 hours to evaluate gene expressions.

Survival Analysis of Neonatal Rat Cardiomyocytes

Neonatal cardiomyocytes (NRCM) were treated with control siRNA or Bsg siRNA for 72 hours, thereafter NRCM were cultured in DMEM without serum for 5 days. NRCM were also cultured in DMEM with recombinant Bsg (1-1000 ng/ml) for 5 days. NRCM survival was examined by the number of residual NRCM in the MTT assay.

Detection of Reactive Oxygen Species in vitro

We treated neonatal rat cardiomyocytes with control IgG (MAB002, R&D, USA) or Bsg inhibitory antibody (UM-8D6 376-020, Ancell, USA) in 2% conditioned medium prepared from *Bsg*^{+/+} cardiac fibroblasts after 24 hours of mechanical stretch. Oxidative stress was measured by 2,7-dichlorofluorescein diacetate (H2DCF-DA) (5 μ mol/L, Molecular Probes, Eugene, OR, USA) for 30 min at 37°C. Presence of ROS was detected as green fluorescence (488 nm) by fluorescence microscopy (BIOREVO, Keyence). The relative fluorescence intensity was measured by Image J.

Cell Proliferation Assay

Mouse CFs were seeded in 96-well plates (2×10^3 cells/well) in 100 μ l DMEM with 10% FBS. On the next day, CFs were stimulated with DMEM containing 5% FBS or 2 % conditioned medium obtained from culture media of cyclic stretch experiment. Human cardiac fibroblasts (hCFs) were purchased from Lonza (Basel, Switzerland). According to the manufacturer, hCFs were isolated from normal adult human ventricle tissue (Basel, Switzerland). hCFs were seeded in 96-well plates (5×10^3 cells/well) in 200 μ l fibroblasts growth medium (FGM) (Lonza, Basel, Switzerland) with 10 nmol/L of either Basigin siRNA or control siRNA. Cells were counted on day 0, 1 and 3, using Cell Titer 96 MTT assay method (Promega, Fitchburg, WI, USA).

Measurement of Cytokine/Chemokine and Growth Factors by Bioplex System

Cytokine/Chemokine and growth factors were evaluated by the Bioplex system according to the manufacturer's instructions (Bio-Rad, Tokyo, Japan). We measured cytokines in conditioned medium from CFs stimulated with cyclic mechanical stretch (10cm² stretch chamber, 5ml DMEM) or AngII (100mm dish, 10ml DMEM). Mouse cytokines/chemokines and growth factors were measured with commercially available kits (Bio-Rad, 9-Plex, MD0-00000EL and 23-Plex, M60-009RDPD). Human cytokines/chemokines and growth factors were measured with commercially available kits (Bio-Rad, 27-Plex, #M50-0KCAF0Y and 21-Plex, #MF0-005KMII).¹² Each experiment was performed in duplicate.

Western Blot Analysis

An equal amount of protein samples were loaded on SDS-PAGE gel and transferred to PVDF membranes (GE Healthcare, UK), and blocked for 1 hour at room temperature in 5 % BSA in Tris-Buffered Saline with Tween 20 (TBST). The primary antibodies used were as follows; Bsg (400:1-1000:1 dilution; R&D systems, AF 772 for mice and AF972 for human), α -tubulin (2000:1, Sigma, T9026), phosphorylated-ERK1/2 (1000:1, Cell Signaling, #9101), and total-ERK1/2 (1000:1, Cell Signaling, #9102), phosphorylated-protein kinase B (Akt) (1000:1, Cell Signaling, #9271), and total-Akt (1000:1, Cell Signaling, #9272), phosphorylated-stress activated protein kinase (SAPK) (1000:1, Cell Signaling, #9251), and total-SAPK (1000:1, Cell Signaling, #9252), CyPA (1:1000 dilution; BIOMOL Research Laboratories, Inc.), GAPDH (1000:1, Santa Cruz, sc-20357), collagen 1a1 (500:1, Santa Cruz, sc-8784), collagen 3a1 (500:1, Santa Cruz, sc-8781), Nox4 (500:1, Santa Cruz, sc-21860), Nox2 (500:1, Santa Cruz, sc-5827). The regions containing proteins were visualized by the enhanced chemiluminescence system (ECL Prime Western Blotting Detection Reagent, GE Healthcare, Buckinghamshire, UK). Densitometric analysis was performed by the Image J Software.

RNA Isolation and Real-time PCR

Isolation of total RNA from mouse heart tissues and NRCM and NRCF were performed using the RNeasy Plus Mini Kit (Qiagen) according to the manufacturer's protocol. Total RNA was converted to cDNA using PrimeScript RT Master Mix (Takara). Primers for murine *Basigin* (Assay ID: Mm01144228_g1) and *Gapdh* (Assay ID: Mm99999915_g1) were purchased from Life Technologies (TaqMan assays, Applied Biosystems, US). Primers for murine *IL-6* (Primer Set ID: MA104898), *TNF- α* (Primer Set ID: MA121221), *IL1- β* (Primer Set ID: MA025939), *Nppa* (Primer Set ID: MA102516), *Nppb* (Primer Set ID: MA103081), *Col1a2* (Collagen I: Primer Set ID: MA128559), *Col3a1* (Collagen III: Primer Set ID: MA131765), *CTGF* (Primer Set ID: MA028643), *Gapdh* (Primer Set ID: MA050371), and primers for rat *Nppa* (Primer Set ID: RA058681), *Nppb* (Primer Set ID: RA043888), *Cybb* (Nox2: Primer Set ID: RA052264), *Nox4* (Primer Set ID: RA064409), *Itgb2* (Integrin β 2: Primer Set ID: RA059368), and *Gapdh* (Primer Set ID: RA015380) were purchased from Takara Bio Inc. (SYBR Green I assays, Shiga, Japan). After reverse transcription, quantitative real-time PCR on the CFX 96 Real-Time PCR Detection System (Bio-Rad) was performed using either SsoFast Probes Supermix (Bio-Rad) for TaqMan probes or SYBR[®] Premix Ex Taq[™] II (Takara) for SYBR probes. The Ct value determined by CFX Manager Software (version2.0, Bio-Rad) for all samples was normalized to

housekeeping gene *Gapdh* and the relative fold change was computed by the $\Delta\Delta\text{Ct}$ method.¹

Clinical Study

The Ethical Review Board of Tohoku University approved the study (#2009-363) and written informed consent was obtained from all participants. We conducted an observational study of the prognostic value of serum soluble Basigin (sBsg) in patients with heart failure who were referred to Tohoku University Hospital for examination. A total of 199 consecutive patients were analyzed for survival rate and first time heart failure re-hospitalization. Serum levels of sBsg in each specific heart disease and association with other inflammatory cytokines were also examined. The clinical characteristics and laboratory data of patients with heart failure are shown in **Supplementary Table I**. The clinical characteristics and laboratory data between patients with high levels of serum Bsg and those with low levels of serum Bsg are shown in **Supplementary Table II**. The cut-off value of serum Bsg between high and low levels was 3,099 ng/ml.

Statistical Analysis in the Clinical Study

Plasma levels of sBsg are presented as mean \pm standard error of the mean (s.e.m.). An unpaired *t*-test was used for comparisons between groups. Event (all cause-death or hospitalization)-free survival curves were generated for both groups. Median follow-up days were 1364 days. In order to identify the cut-off points of high and low sBsg groups, we performed survival classification and regression trees (survival CART) analyses. All reported P values are 2-tailed, with a P value of less than 0.05 indicating statistical significance. Analyses were performed in SPSS, version 19.0 (Chicago, IL, USA) and R version 3.1.3 with the rpart package.¹⁸

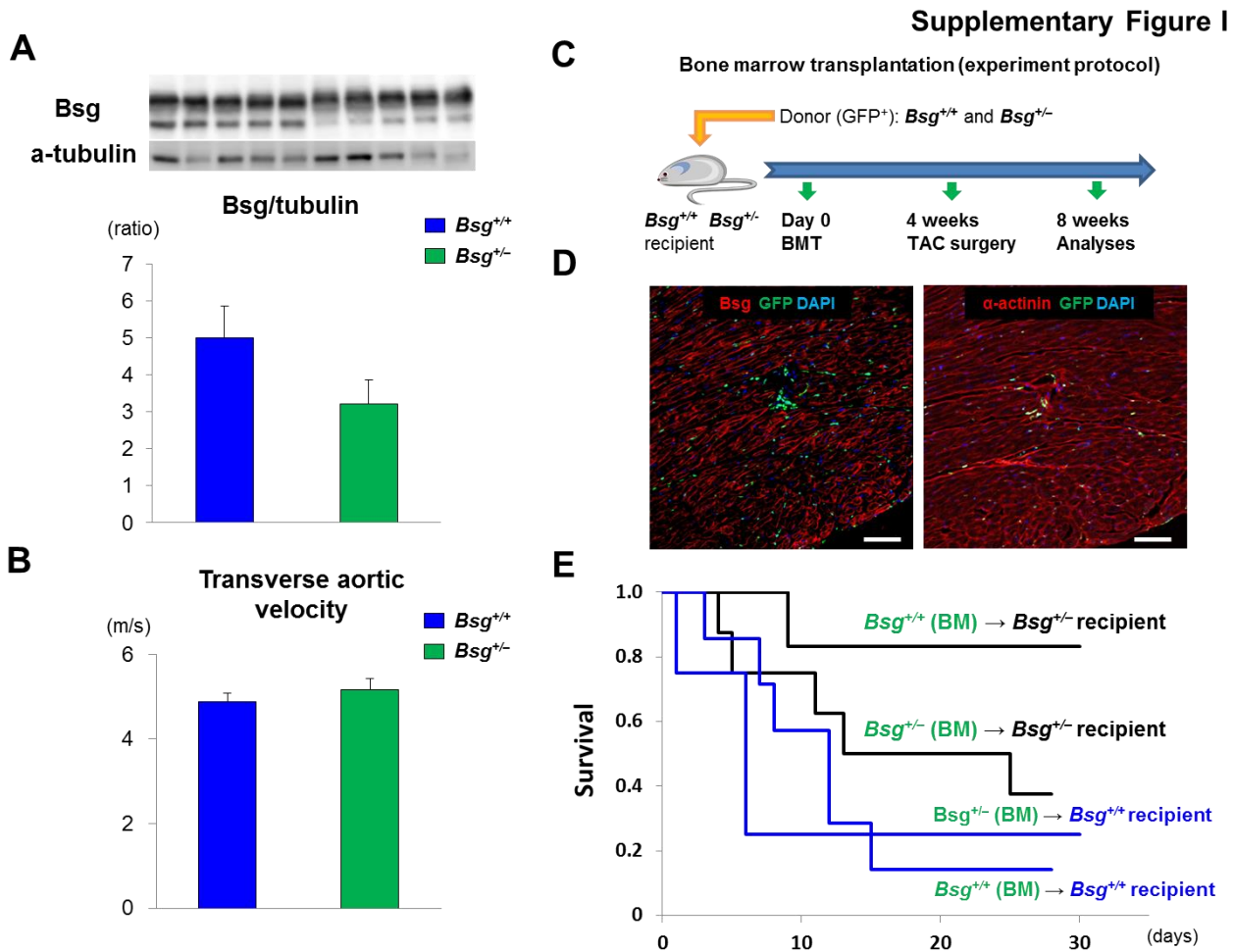
Statistical Analysis for *in Vivo* and *in Vitro* Study

Statistical analysis was performed with GraphPad Prism, version 6 (GraphPad Software Inc, California, USA). Results are shown as mean \pm standard error of the mean (s.e.m) for all studies. Comparisons of means between 2 groups were performed by unpaired *t*-test. Comparisons of mean parameters among multiple groups were made by one-way or two-way analysis of variance (ANOVA), followed by Bonferroni's multiple comparisons tests. $P < 0.05$ was considered to be statistically significant.^{12, 13}

References

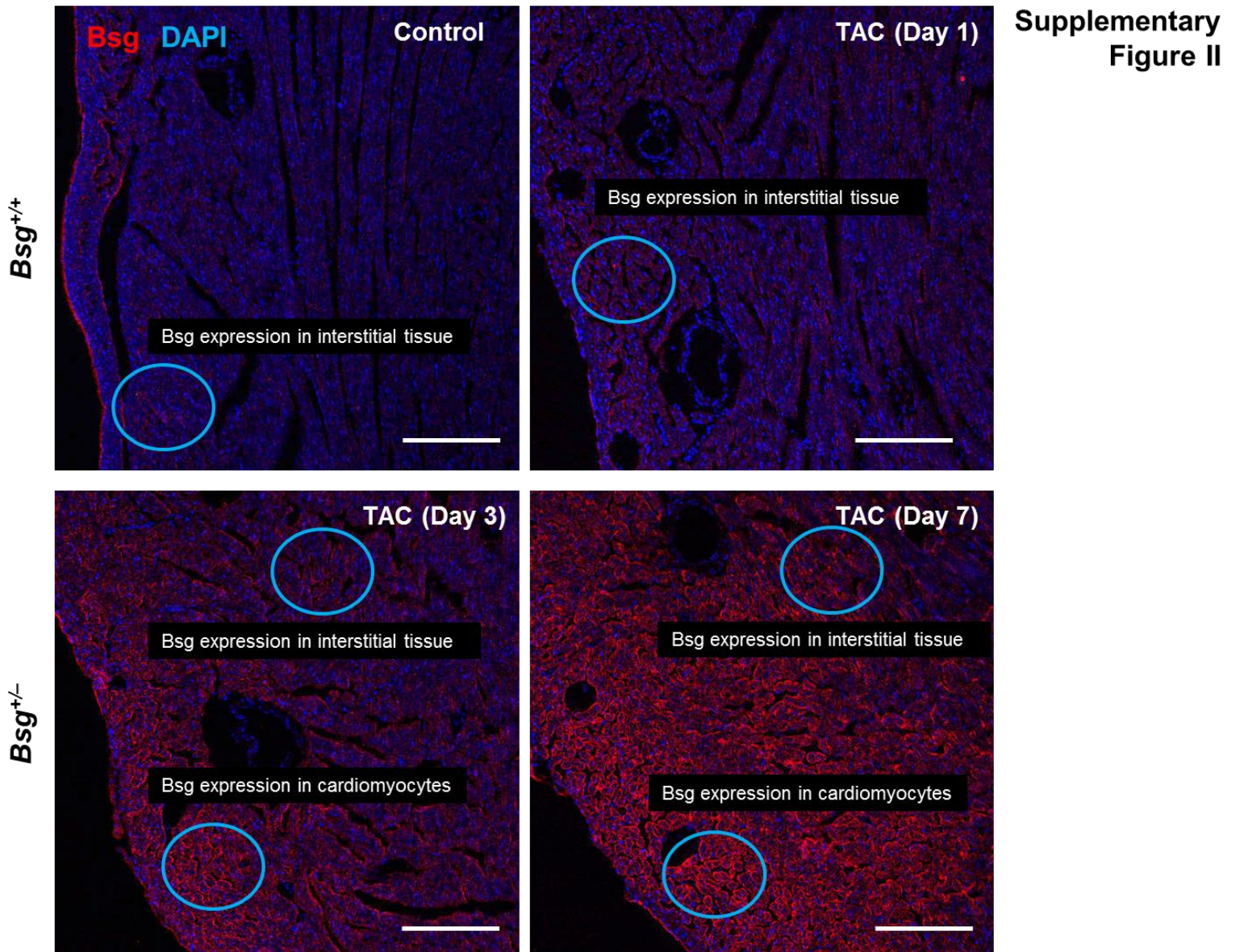
1. Ikeda S, Satoh K, Kikuchi N, Miyata S, Suzuki K, Omura J, Shimizu T, Kobayashi K, Kobayashi K, Fukumoto Y, Sakata Y, Shimokawa H. Crucial role of rho-kinase in pressure overload-induced right ventricular hypertrophy and dysfunction in mice. *Arterioscler Thromb Vasc Biol.* 2014;34:1260-71.
2. Hu P, Zhang D, Swenson L, Chakrabarti G, Abel ED, Litwin SE. Minimally invasive aortic banding in mice: Effects of altered cardiomyocyte insulin signaling during pressure overload. *Am J Physiol Heart Circ Physiol.* 2003;285:H1261-9.
3. Asaumi Y, Kagaya Y, Takeda M, Yamaguchi N, Tada H, Ito K, Ohta J, Shiroto T, Shirato K, Minegishi N, Shimokawa H. Protective role of endogenous erythropoietin system in nonhematopoietic cells against pressure overload-induced left ventricular dysfunction in mice. *Circulation.* 2007;115:2022-32.
4. Kato N, Yuzawa Y, Kosugi T, Hobo A, Sato W, Miwa Y, Sakamoto K, Matsuo S, Kadomatsu K. The e-selectin ligand basigin/CD147 is responsible for neutrophil recruitment in renal ischemia/reperfusion. *J Am Soc Nephrol.* 2009;20:1565-76.
5. Kuno N, Kadomatsu K, Fan Q-W, Hagihara M, Senda T, Mizutani S, Muramatsu T. Female sterility in mice lacking the basigin gene, which encodes a transmembrane glycoprotein belonging to the immunoglobulin superfamily. *FEBS Letters.* 1998;425:191-194.
6. Igakura T, Kadomatsu K, Kaname T, Muramatsu H, Fan QW, Miyauchi T, Toyama Y, Kuno N, Yuasa S, Takahashi M, Senda T, Taguchi O, Yamamura K, Arimura K, Muramatsu T. A null mutation in basigin, an immunoglobulin superfamily member, indicates its important roles in peri-implantation development and spermatogenesis. *Dev Biol.* 1998;194:152-65.
7. Zavadzka JA, Plyler RA, Bouges S, Koval CN, Rivers WT, Beck CU, Chang EI, Stroud RE, Mukherjee R, Spinale FG. Cardiac-restricted overexpression of extracellular matrix metalloproteinase inducer causes myocardial remodeling and dysfunction in aging mice. *Am J Physiol Heart Circ Physiol.* 2008;295:H1394-402.
8. Nakano M, Satoh K, Fukumoto Y, Ito Y, Kagaya Y, Ishii N, Sugamura K, Shimokawa H. Important role of erythropoietin receptor to promote VEGF expression and angiogenesis in peripheral ischemia in mice. *Circ Res.* 2007;100:662-9.
9. Satoh K, Kagaya Y, Nakano M, et al. Important role of endogenous erythropoietin system in recruitment of endothelial progenitor cells in hypoxia-induced pulmonary hypertension

- in mice. *Circulation*. 2006;113:1442-50.
10. Satoh K, Nigro P, Matoba T, O'Dell MR, Cui Z, Shi X, Mohan A, Yan C, Abe J, Illig KA, Berk BC. Cyclophilin A enhances vascular oxidative stress and the development of angiotensin ii-induced aortic aneurysms. *Nat Med*. 2009;15:649-56.
 11. Nigro P, Satoh K, O'Dell MR, Soe NN, Cui Z, Mohan A, Abe J, Alexis JD, Sparks JD, Berk BC. Cyclophilin A is an inflammatory mediator that promotes atherosclerosis in apolipoprotein E-deficient mice. *J Exp Med*. 2011;208:53-66.
 12. Satoh K, Satoh T, Kikuchi N, et al. Basigin mediates pulmonary hypertension by promoting inflammation and vascular smooth muscle cell proliferation. *Circ Res*. 2014;115:738-50.
 13. Satoh K, Nigro P, Zeidan A, Soe NN, Jaffre F, Oikawa M, O'Dell MR, Cui Z, Menon P, Lu Y, Mohan A, Yan C, Blaxall BC, Berk BC. Cyclophilin A promotes cardiac hypertrophy in apolipoprotein E-deficient mice. *Arterioscler Thromb Vasc Biol*. 2011;31:1116-23.
 14. Takefuji M, Kruger M, Sivaraj KK, Kaibuchi K, Offermanns S, Wettschureck N. Rhogef12 controls cardiac remodeling by integrating G protein- and integrin-dependent signaling cascades. *J Exp Med*. 2013;210:665-73.
 15. Herum KM, Lunde IG, Skrbic B, Florholmen G, Behmen D, Sjaastad I, Carlson CR, Gomez MF, Christensen G. Syndecan-4 signaling via nfat regulates extracellular matrix production and cardiac myofibroblast differentiation in response to mechanical stress. *J Mol Cell Cardiol*. 2013;54:73-81.
 16. Satoh K, Matoba T, Suzuki J, O'Dell MR, Nigro P, Cui Z, Mohan A, Pan S, Li L, Jin ZG, Yan C, Abe J, Berk BC. Cyclophilin A mediates vascular remodeling by promoting inflammation and vascular smooth muscle cell proliferation. *Circulation*. 2008;117:3088-98.
 17. Funayama A, Shishido T, Netsu S, Narumi T, Kadowaki S, Takahashi H, Miyamoto T, Watanabe T, Woo CH, Abe J, Kuwahara K, Nakao K, Takeishi Y, Kubota I. Cardiac nuclear high mobility group box 1 prevents the development of cardiac hypertrophy and heart failure. *Cardiovasc Res*. 2013;99:657-64.
 18. R TR. A language and environment for statistical computing. . *R Foundation for Statistical Computing, Vienna, Austria*. URL <http://www.R-project.org/>.



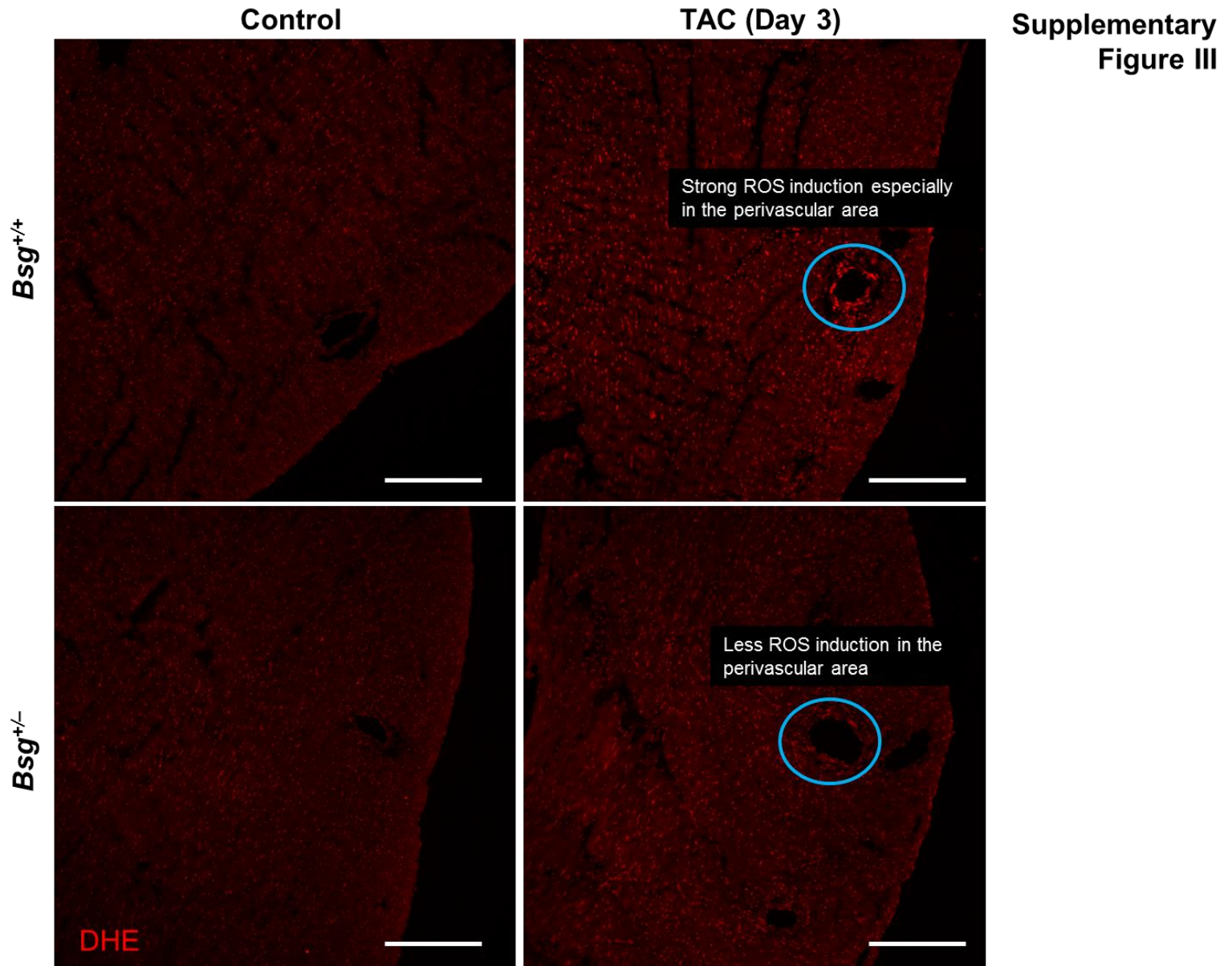
Supplementary Figure I. *Bsg* in cardiac tissue plays a crucial role for pressure overload-induced heart failure

(A) Representative Western blotting photographs of Basigin (*Bsg*) and quantitative analysis in *Bsg*^{+/-} mice and *Bsg*^{+/+} mice at baseline ($n = 4$ each). (B) Transverse aortic velocity in *Bsg*^{+/-} and *Bsg*^{+/+} mice at 4 weeks after TAC ($n = 8$ in each group). (C) Bone marrow transplantation (BMT) protocol. *Bsg*^{+/-} and *Bsg*^{+/+} bone marrow (BM) were transplanted into irradiated 8-week-old *Bsg*^{+/-} and *Bsg*^{+/+} mice. After 4 weeks, *Bsg*^{+/-} and *Bsg*^{+/+} mice were subjected to transverse aortic constriction (TAC) and were thereafter followed for 4 weeks. (D) Representative photomicrographs of immunostaining showing localization of GFP-positive (green fluorescent protein) cells in the heart from *Bsg*^{+/+} recipient mice with *Bsg*^{+/+} GFP positive BM (green) 4 weeks after TAC. *Bsg* (red) and α -actinin (red). There were few numbers of GFP/*Bsg* double positive cells in pressure-overloaded heart tissue. Scale bars, 100 μ m. (E) Long-term survival curves demonstrated that *Bsg*^{+/-} recipient mice were more likely to survive compared with *Bsg*^{+/+} recipient mice, regardless of the source of BM (*Bsg*^{+/+} or *Bsg*^{+/-} BM) (*Bsg*^{+/+} recipient mice with *Bsg*^{+/+} BM: $n = 7$; *Bsg*^{+/-} recipient mice with *Bsg*^{+/+} BM: $n = 6$; *Bsg*^{+/+} recipient mice with *Bsg*^{+/-} BM: $n = 4$; *Bsg*^{+/-} recipient mice with *Bsg*^{+/-} BM: $n = 6$). Results are expressed as mean \pm s.e.m. * $P < 0.05$.



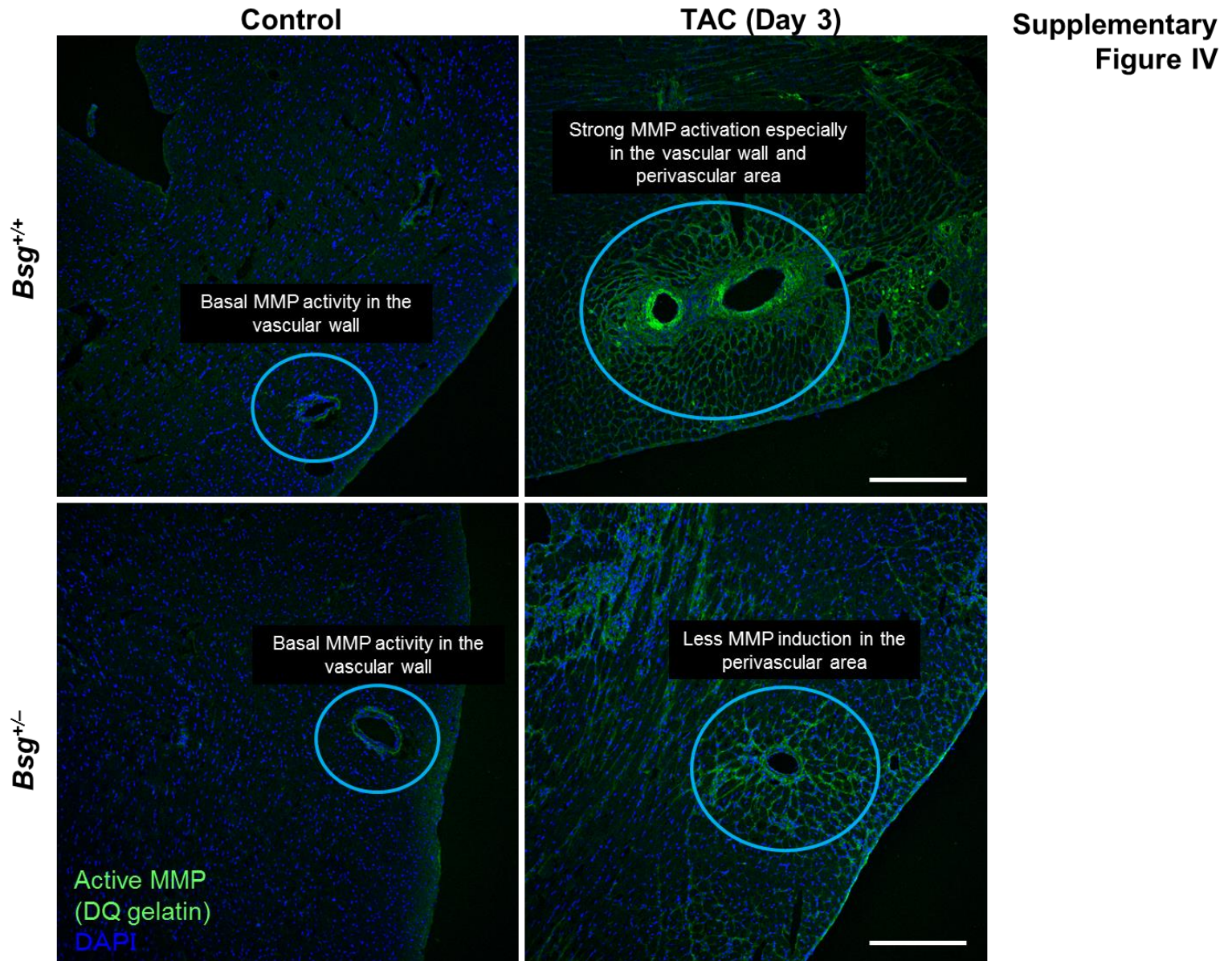
Supplementary Figure II. Pressure overload-induced Bsg expression in cardiomyocytes

Representative immunostaining of the left ventricle (LV) after transverse aortic constriction (TAC). Bsg (Alexa Fluor-563, red) and DAPI (blue) expression in the LV after TAC. The expression of Bsg was strong in interstitial tissue and cardiomyocytes. TAC induced Bsg expression in the LV in a time-dependent manner, especially on the surface of cardiomyocytes. Scale bars, 200 μ m.



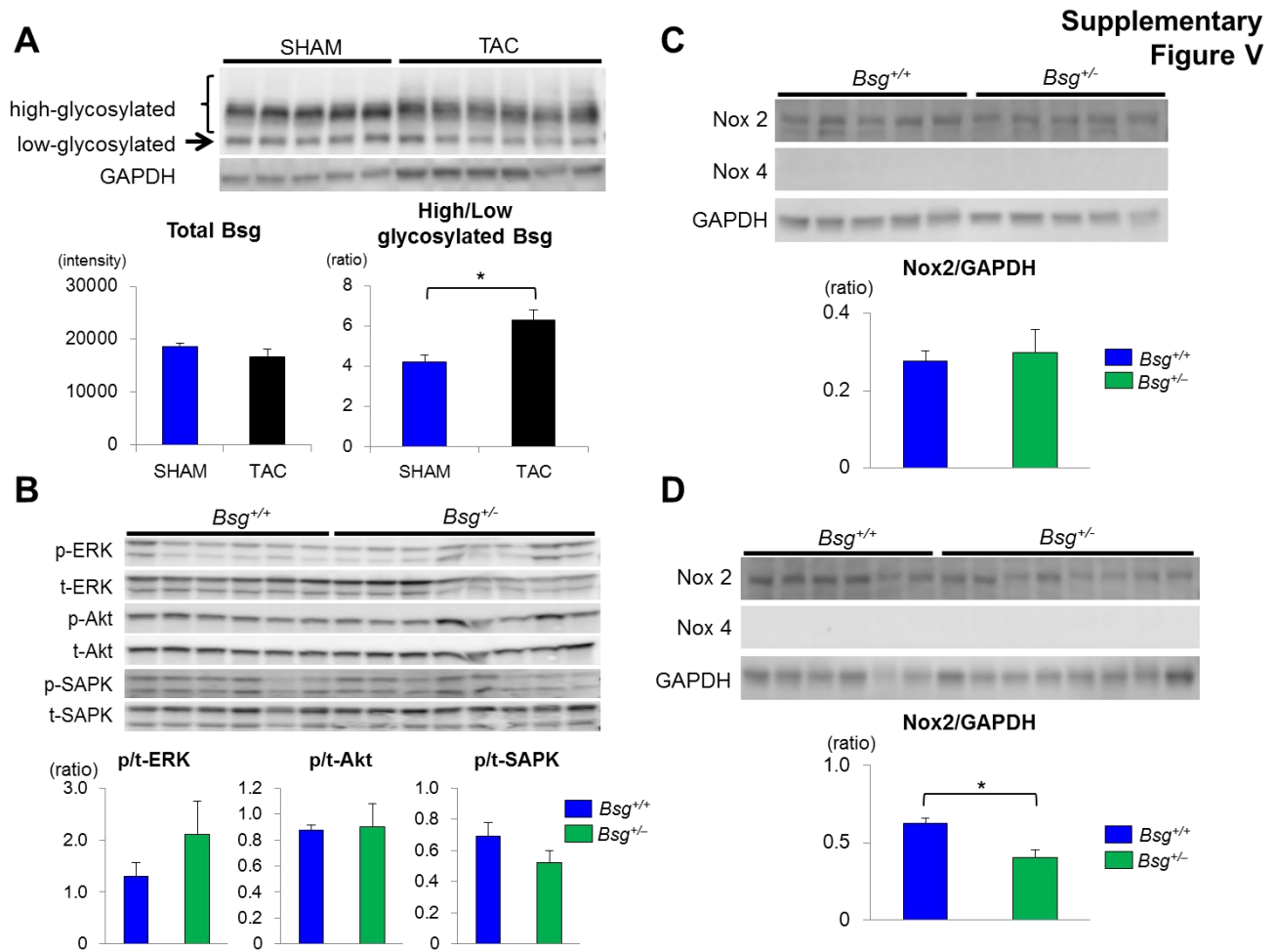
Supplementary Figure III. Bsg augments pressure overload-induced oxidative stress

Representative immunostaining of the left ventricles (LV) after transverse aortic constriction (TAC). Representative pictures of dihydroethidium (DHE) staining of *Bsg*^{+/-} and *Bsg*^{+/+} LV after TAC. Scale bars, 300 μ m. Pressure overload-induced reactive oxygen species (ROS) was less in *Bsg*^{+/-} LV compared with *Bsg*^{+/+} after TAC.



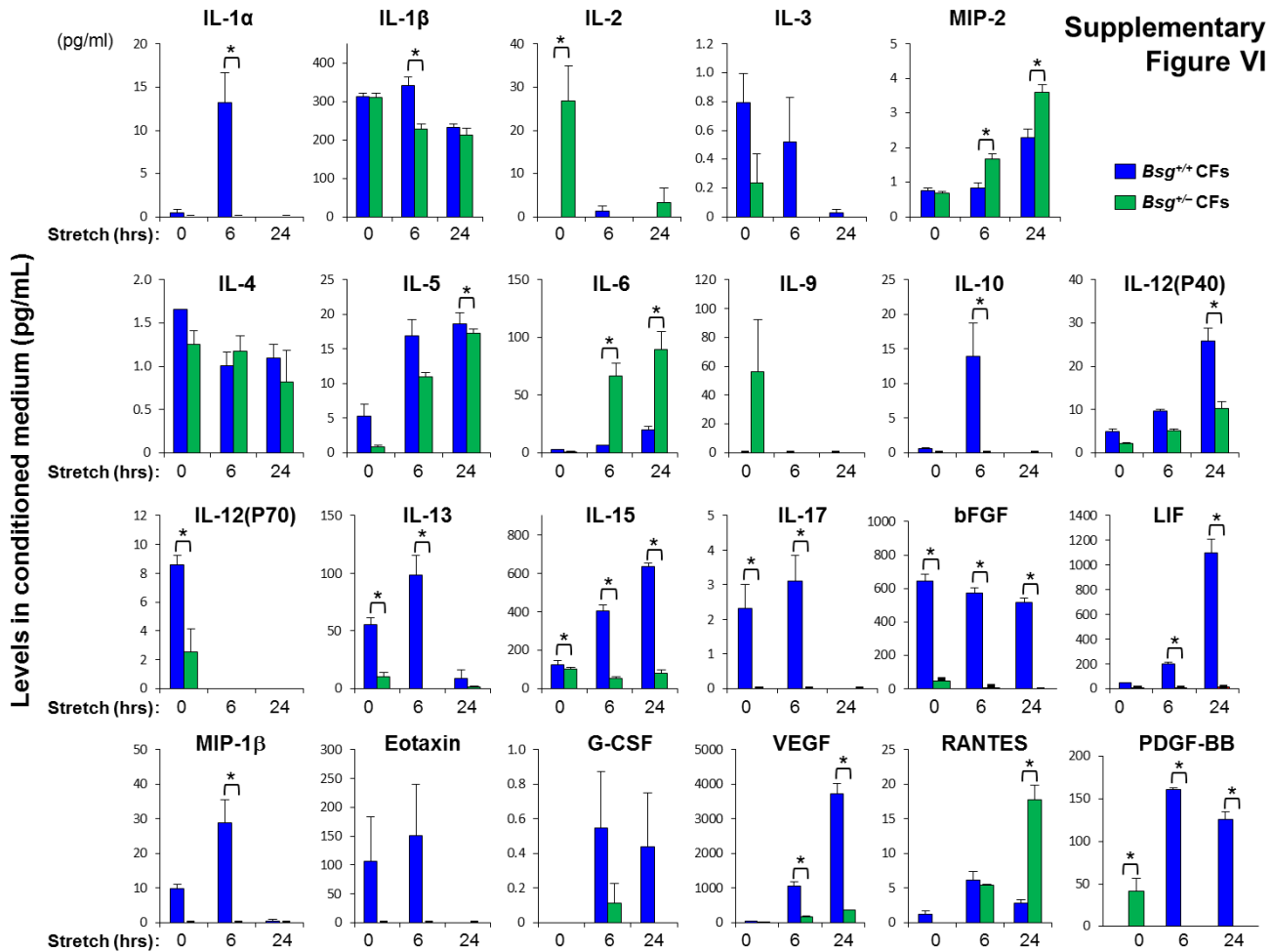
Supplementary Figure IV. Bsg augments pressure overload-induced MMP activation

Representative pictures of *in situ* zymography (DQ gelatin) for gelatinase activities in *Bsg*^{+/-} and *Bsg*^{+/+} LV after TAC. Pressure overload-induced MMP activation was strong especially in perivascular area in *Bsg*^{+/+} LV, which was less in *Bsg*^{+/-} LV after TAC. Scale bars, 300 μ m.



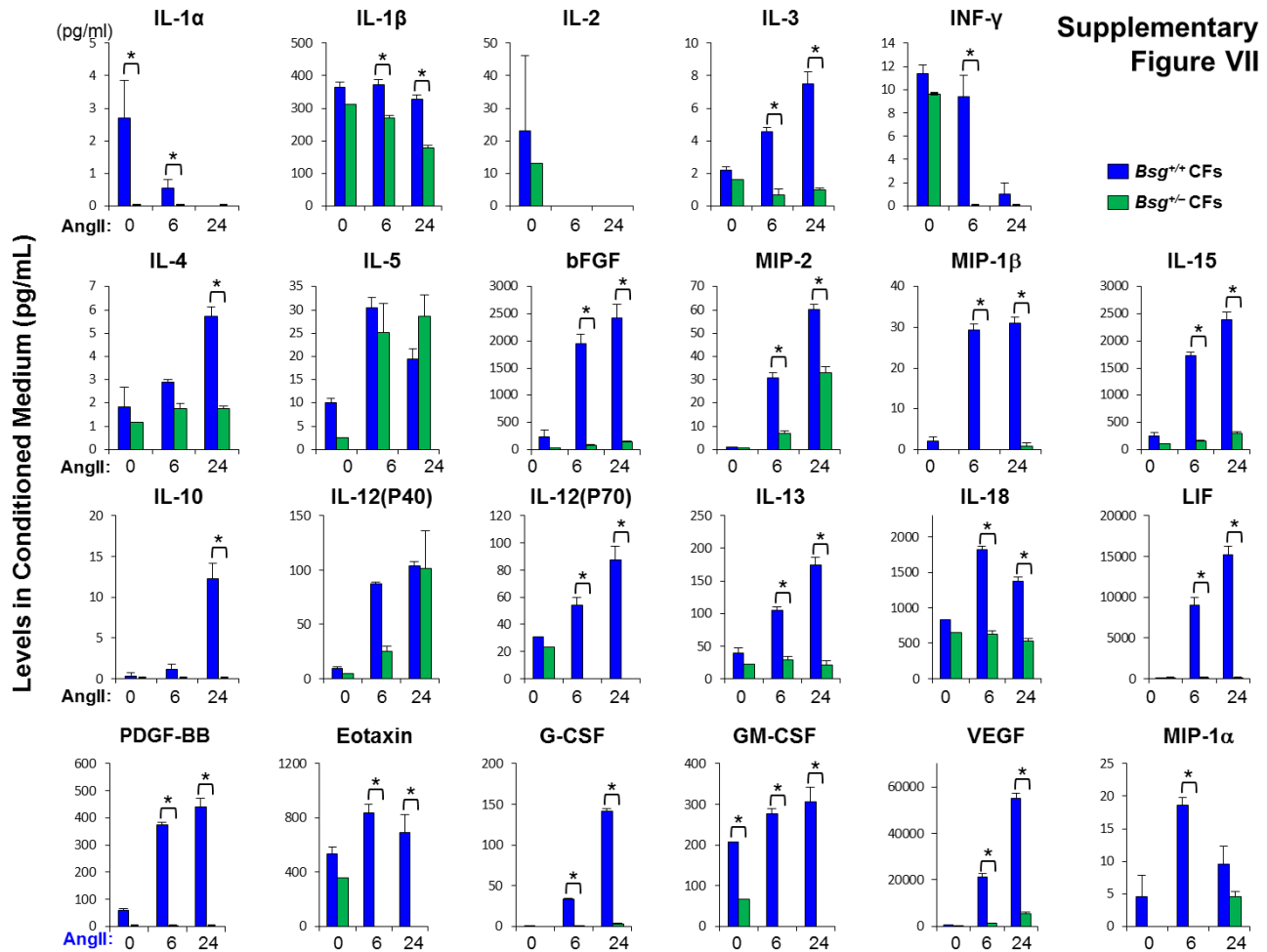
Supplementary Figure V. Bsg mediated cell signaling in Vivo by pressure overload.

(A) Quantitative Western blotting analysis of Bsg in heart homogenates in *Bsg*^{+/+} mice at 1 week after TAC (n = 5-6). (B) Quantitative Western blotting of ERK, Akt and SAPK in heart homogenates of *Bsg*^{+/-} and *Bsg*^{+/+} mice at 1 week after TAC (n = 6-8). (C) Quantitative Western blotting analysis of Nox2 and Nox4 expression in heart homogenates of *Bsg*^{+/+} and *Bsg*^{+/-} at baseline (n = 5 each). (D) Quantitative Western blotting analysis of Nox2 and Nox4 expression in heart homogenates of *Bsg*^{+/+} and *Bsg*^{+/-} at 1 week after TAC (n = 6-8). Results are expressed as mean ± s.e.m. **P*<0.05.



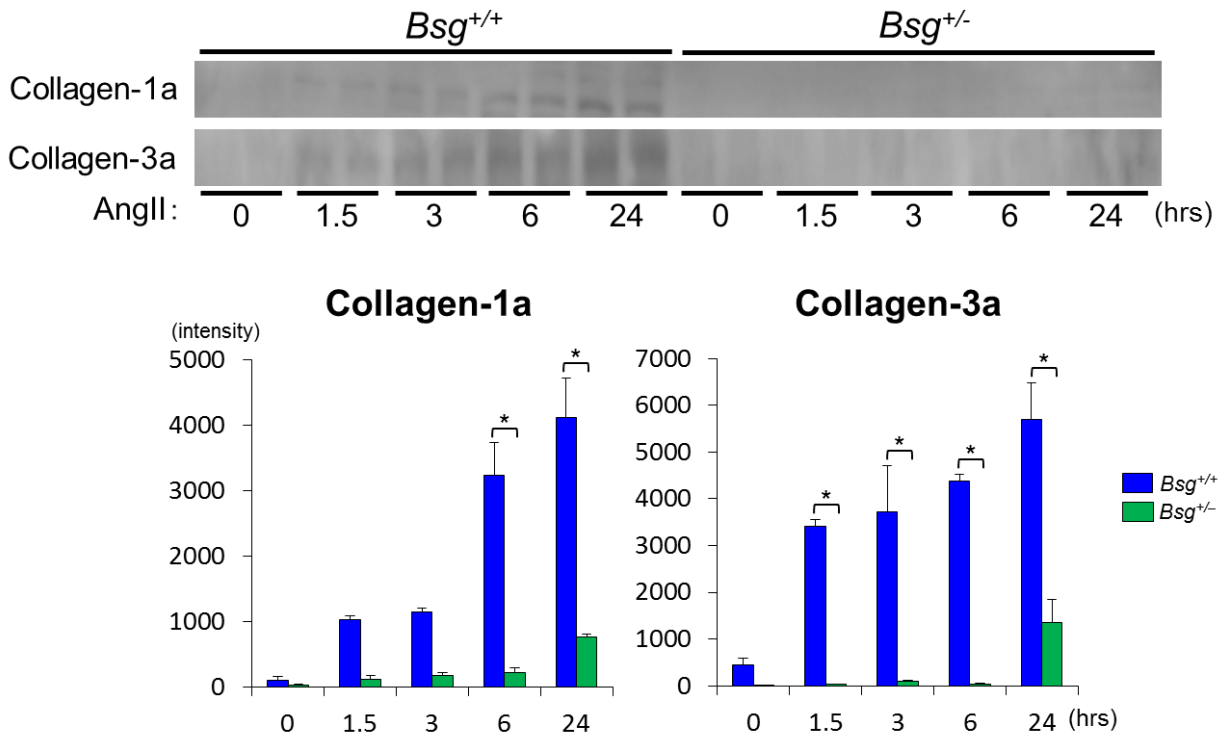
Supplementary Figure VI. *Bsg* promotes secretion of inflammatory cytokines/chemokines and growth factors from cardiac fibroblasts in response to mechanical stretch

Bsg^{+/-} and *Bsg*^{+/+} cardiac fibroblasts (CFs) were subjected to mechanical cyclic stretch at 1 Hz with 20 % elongation for 0, 6 and 24 hours ($n = 4$ each), and then conditioned medium (CM) were analyzed by Bio-plex cytokines array system. Levels of cytokines/chemokines and growth factors secreted from *Bsg*^{+/-} and *Bsg*^{+/+} CFs. Results are expressed as mean \pm s.e.m. * $P < 0.05$.

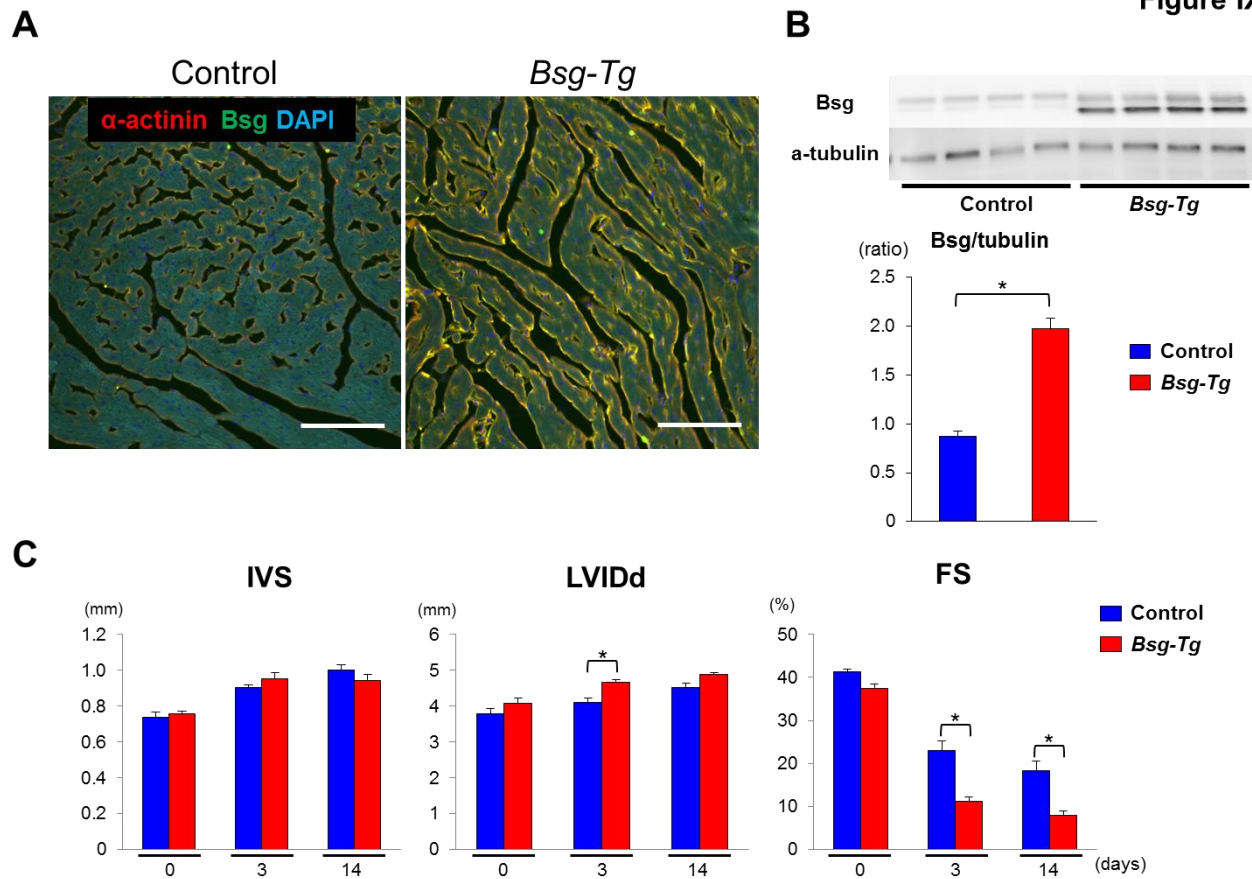


Supplementary Figure VII. *Bsg* promotes secretion of inflammatory cytokines/chemokines and growth factors from cardiac fibroblasts in response to angiotensin II

Bsg^{+/-} and *Bsg*^{+/+} CFs were stimulated with AngII (100 nmol/l) for 0, 1.5, 3, 6 and 24 hours ($n = 3$ each), and then conditioned medium (CM) were analyzed by the Bio-plex cytokines array system. Levels of cytokines/chemokines and growth factors secreted from *Bsg*^{+/-} and *Bsg*^{+/+} CFs. Results are expressed as mean \pm s.e.m. * $P < 0.05$.

Supplementary
Figure VIII**Supplementary Figure VIII. Bsg promotes collagen synthesis in cardiac fibroblasts.**

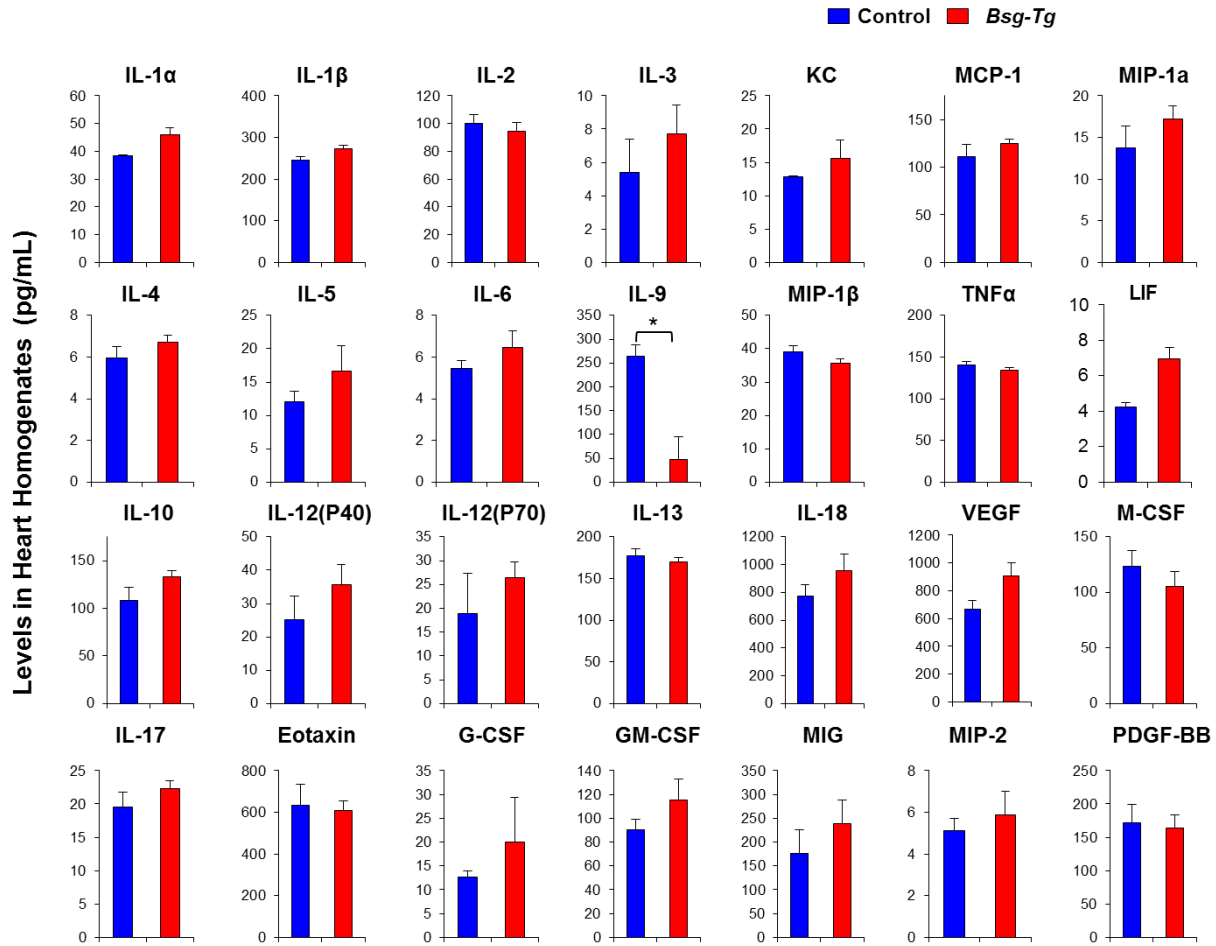
Bsg^{+/-} and *Bsg*^{+/+} cardiac fibroblasts (CFs) were subjected to AngII (100nM) for 0, 1.5, 3, 6 and 24 hours (n = 2 each) and then conditioned medium (CM) were collected. Quantitative Western blotting analyses of collagen-1a and collagen-3a in CM. Results are expressed as mean ± s.e.m. *P < 0.05.

Supplementary
Figure IX

Supplementary Figure IX. Cardiomyocyte-specific Bsg overexpressing mice shows markedly worsened cardiac function after TAC.

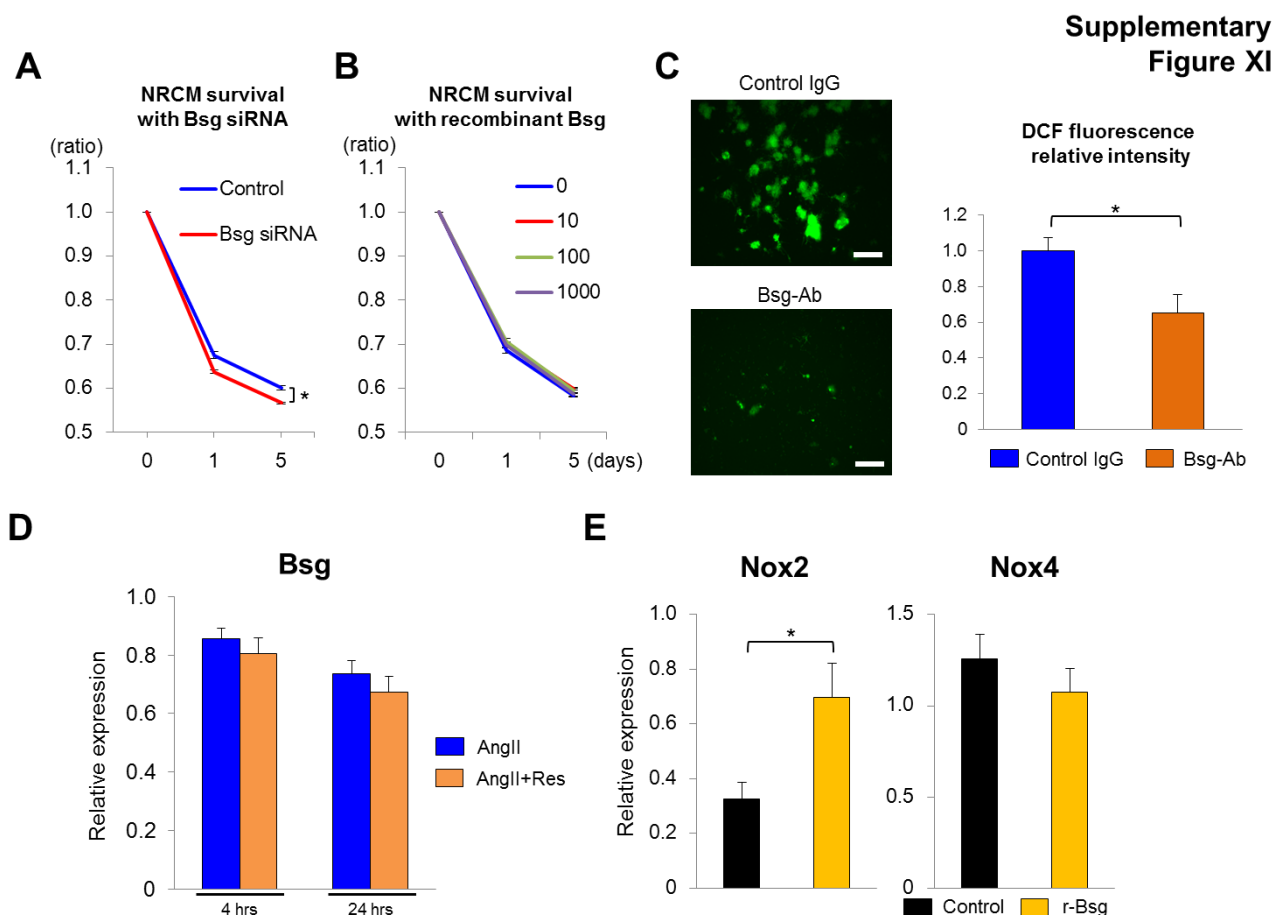
(A) Representative photomicrograph of immunostaining showing localization of Bsg (Alexa Fluor-488, green) in heart from *Bsg-Tg* mice and littermate control at baseline. Bsg (green), α -actinin (red) and DAPI (blue). Scale bars, 100 μ m. (B) Representative pictures of Bsg expression in heart homogenates in *Bsg-Tg* mice and littermate controls at baseline, and quantitative analysis of them (n=4 each). (C) Quantitative analysis of the parameters of cardiac function in *Bsg-Tg* mice and littermate controls at days 0, 3, 14 after TAC (n = 4-5). IVS, interventricular septum thickness; LVIDd, LV internal end-diastolic diameter; LVFS, LV fractional shortening. Results are expressed as mean \pm s.e.m. * P <0.05

Supplementary Figure X



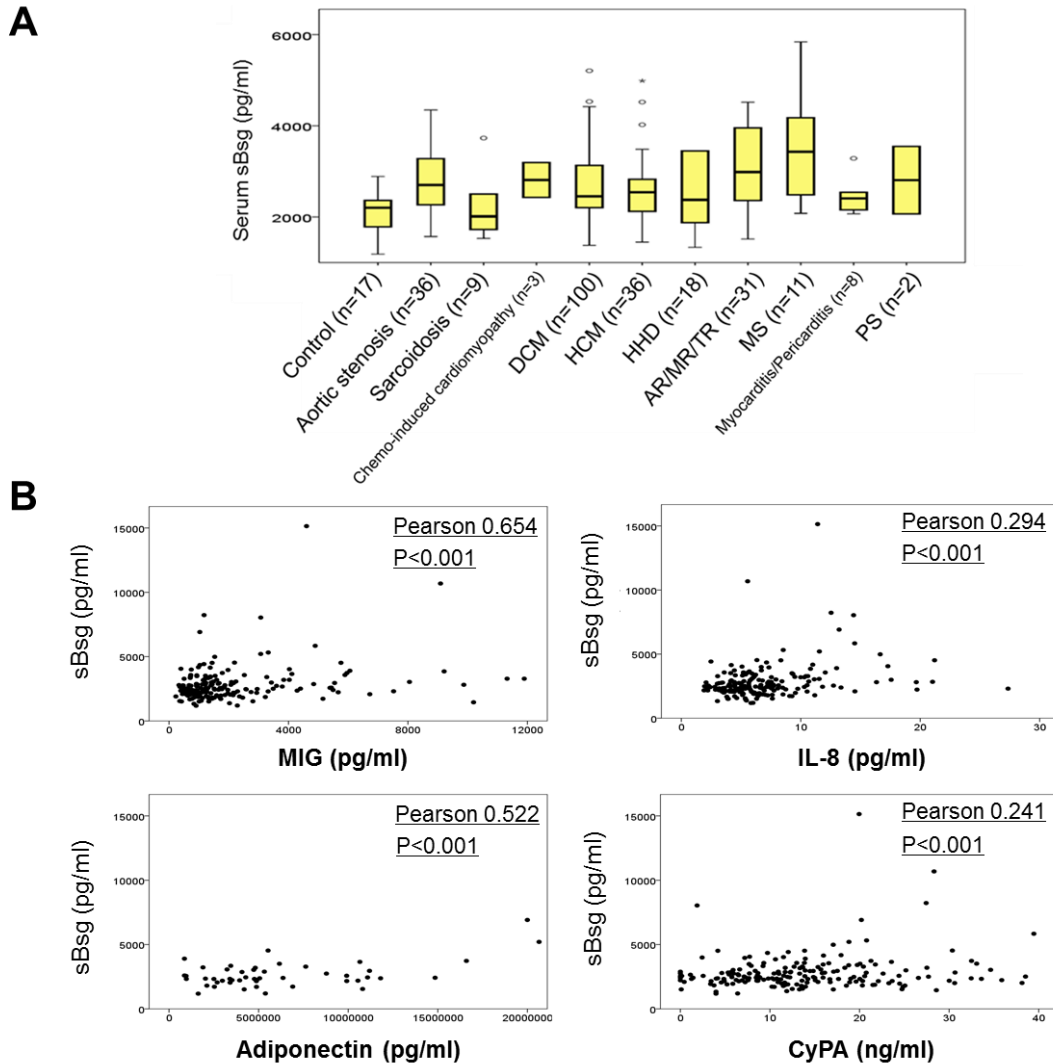
Supplementary Figure X. Baseline characteristics of cytokines arrays in cardiomyocyte-specific *Bsg* overexpressing hearts

Baseline characteristics of cardiomyocyte-specific *Bsg* overexpressing hearts (*Bsg-Tg*) and littermate controls. Heart tissue homogenates samples were analyzed by Bio-plex cytokines array system. Levels of cytokines/chemokines and growth factors in the hearts from *Bsg-Tg* and control mice ($n = 3$). Results are expressed as mean \pm s.e.m. * $P < 0.05$.



Supplementary Figure XI. Association between Bsg and oxidative stress in neonatal rat cardiomyocytes.

Neonatal rat cardiomyocytes (NRCM) survival assay by Cell Titer 96 MTT assay. (A) NRCM was transfected with Bsg siRNA or control siRNA for 72 hours, thereafter cultured in DMEM without serum for 5 days ($n = 8$ in each group). (B) NRCM was cultured in DMEM with recombinant Bsg for 5 days ($n = 8$ in each group). (C) Representative photomicrograph of oxidative stress in NRCM at 4 hours, which were treated with control IgG or inhibitory antibody to Bsg (Bsg-Ab) in 2% conditioned medium prepared from *Bsg*^{+/+} cardiac fibroblasts after 24 hours of mechanical stretch. Oxidative stress was measured by dichlorofluorescein (DCF) assay. Bar graphs show the relative intensity of DCF fluorescence ($n = 4$ in each group). (D) Relative mRNA expressions of Bsg in NRCM treated with AngII (100 nmol/l) with or without resveratrol (Res, 25 μmol/l) for up to 24 hours ($n = 6$ in each group). (E) Relative mRNA expressions of Nox2 and Nox4 in NRCM treated with hrBsg (1 μg/ml, 24 hours) ($n = 6$ in each group). Results are expressed as mean \pm s.e.m. * $P < 0.05$.

Supplementary
Figure XII

Supplementary Figure XII. Serum levels of Bsg as a novel prognostic biomarker for patients with heart failure

(A) Serum levels of sBsg according to the specific diagnosis of heart diseases. Serum sBsg were increased in several pressure overloaded-heart diseases, such as aortic valve stenosis (AS), hypertrophic cardiomyopathy (HCM), hypertensive heart disease (HHD), aortic valve regurgitation (AR), mitral valve regurgitation (MR), tricuspid valve regurgitation (TR), mitral valve stenosis (MS), and pulmonary valve stenosis (PS). (B) Correlations between serum sBsg levels and inflammatory cytokines. Serum levels of Bsg were significantly correlated with those of monokine induced by gamma interferon (MIG), IL-8, adiponectin and cyclophilin A (CyPA).

**Supplementary
Table I**

	Control (n=8)	HF (n=120)
Age (years)	53±9	60±14
Male (%)	16.7	64.1
Body mass index (kg/m ²)	23.0±2.0	23.5±4.7
BNP (pg/ml)	24.9±20.9	417.2±690.3
WHO class		
I & II (%)	100	74.5
III (%)	0	17.6
IV (%)	0	7.8
echocardiography		
LAD (mm)	31.4±4.3	43.2±10.3
LVDd (mm)	44.6±2.2	51.6±10.5
LVDs (mm)	27.5±1.1	36.3±12.8
EF (%)	66.6±5.8	56.9±17.1
Medical history		
Hypertension (%)	33.3	45.6
Diabetes mellitus (%)	66.7	21.4
Dislipidemia (%)	66.7	24.3
Medication		
ACE-I (%)	0	36.9
ARB (%)	33.3	33
β-blocker (%)	33.3	56.3
CCB (%)	16.7	30.1

Supplementary Table I. The clinical characteristics and laboratory data of patients with heart failure.

Results are expressed as mean ± SD.

Heart failure (HF), brain natriuretic peptide (BNP), left atrial diameter (LAD), left ventricle end-diastolic diameter (LVDd), left ventricle end-systolic diameter (LVDs), ejection fraction (EF), angiotensin converting enzyme inhibitor (ACE-I), angiotensin receptor blocker (ARB), calcium channel blocker (CCB).

Supplementary Table II

Serum Bsg	High (n=37)	Low (n=83)
Age (years)	60.6±14.1	58.3±18.9
Male (%)	62.7	67.9
Body mass index (kg/m ²)	23.0±3.5	24.7±6.4
BNP (pg/ml)	304.0±566.5	656.6±870.6
WHO class		
I / II (%)	60.7	79.7
III (%)	21.4	16.2
IV (%)	17.9	4.1
echocardiography		
LAD (mm)	40.6±8.3	47.2±12.8
LVDd (mm)	50.7±10.0	53.3±11.0
LVDs (mm)	35.4±13.0	38.2±11.9
EF (%)	57.7±17.4	56.7±15.8
Medical history		
Hypertension (%)	41.3	57.1
Diabetes mellitus (%)	16.0	35.7
Dislipidemia (%)	29.3	10.7
Medication		
ACE-I (%)	36.0	39.3
ARB (%)	28.0	46.4
β-blocker (%)	57.3	53.6
CCB (%)	29.3	32.1

Supplementary Table II. The clinical characteristics and laboratory data between patients with high levels of serum Bsg and those with low levels of serum Bsg

Results are expressed as mean ± SD.

Brain natriuretic peptide (BNP), left atrial diameter (LAD), left ventricle end-diastolic diameter (LVDd), left ventricle end-systolic diameter (LVDs), ejection fraction (EF), angiotensin converting enzyme inhibitor (ACE-I), angiotensin receptor blocker (ARB), calcium channel blocker (CCB).